Electrostatic Bubbles and Supramolecular Assistance of Photosensitization by Carboxylated Ru(II) Complexes

Pierre G. Potvin,* Phuong Uyen Luyen, and Jan Bräckow[†]

Contribution from the Department of Chemistry, York University, 4700 Keele Street, Toronto, ON, Canada M3J 1P3

Received September 24, 2002; E-mail: pgpotvin@yorku.ca

Abstract: The paper examines the supramolecular effects at play during photosensitization by carboxylated Ru^{II} sensitizers, both by experiment and by modeling. Experimentally, twelve Ru^{II} complexes of pyrazolylpyridine and polypyridine ligands, including two benchmark complexes and two new species, were assessed as photosensitizers by measurement of the kinetics of methyl viologen cation radical ($MV^{\bullet+}$) generation through an oxidative, photoinduced electron transfer (PET) to methyl viologen (MV^{2+}) under continuous irradiation in the presence of a sacrificial reductant. All complexes, luminescent or not, produced measurable amounts of $MV^{\bullet+}$ in CH_3CN. The assessment protocol was found to be useful with sensitizers of widely varying excited-state lifetimes (τ) as well as being easier and faster than conventional approaches. The seven sensitizers bearing peripheral COOH groups were found to be significantly more active than their non-carboxylated analogues, which is consistent with ionization of the COOH groups and electrostatic promotion of PET. Only the luminescent complexes were active in aqueous solvents, where τ appears to be the dominant effector. The benefits are exemplified by the singly carboxylated $[Ru(H\mathbf{1})(bpy)_2]^{2+}$ (H**1** is 1-(4-carboxyphenyl)-3-(2-pyridyl)-4,5,6,7-tetrahydroindazole), a weakly luminescent sensitizer that was less active in aqueous solvents than $[Ru(bpy)_3]^{2+}$ (bpy is 2,2′-bipyridine), but which became the better sensitizer in CH_3CN. Computationally, electrostatic field and dissociation energy calculations demonstrated that even a single peripheral COO^- substituent suffices to provide supramolecular assistance: it defines a spheric "bubble" of electrostatically attractive space that is sufficiently large to allow the supramolecular preassociation of MV^{2+}, which provides an entropic advantage to PET that reduces the importance of τ in organic solvent. Calculations also show that the PET is electrostatically favored over its reverse (BET) even with cationic sensitizers because the "bubble" contracts after PET while the bulk medium becomes more repulsive, and favorable cation exchanges can occur to effect post-PET dissociation. Two peripheral COO^- groups can define a two-point binding site for MV^{2+} in an attractive sector of space that contracts to a kidney-shaped "bubble" after PET. This enables unimolecular PET while the reverse reaction remains bimolecular. The resultant benefits are illustrated with $[Ru(Na\mathbf{1})_2(bpy)]^{2+}$, a very weakly luminescent sensitizer that was totally inactive in H_2O but appreciably active in CH_3CN, despite the need to displace Na^+ in order to derive any electrostatic benefit. The Marcus free energies of activation for PET and BET corroborate the benefits of carboxylation, solvent, and other factors and correlated with the experimental rate constants.

1. Introduction

Ru^{II}-based photosensitizers continue to hold promise in solar energy capture,[1] but the design and identification of promising candidates have posed continuing challenges to the implementation of photoredox systems. With respect to the latter, we have recently developed an expedient method for the comparative assessment of sensitization ability,[2] one that avoids the laborious determination of a sensitizer's fundamental photophysical properties. We have since applied this method to the assessment

of a few new candidates in comparisons with well-known materials under identical conditions.[3−5] With respect to the problem of design, we have endeavored to address two of the basic issues plaguing Ru^{II}-based sensitizers, namely unfavorable electrostatics and photoproduct separation.

The best studied Ru-based sensitizer is $[Ru(bpy)_3]^{2+}$ (bpy is 2,2′-bipyridine),[6,7] which displays useful light absorption and redox properties. Its photoinduced electron-transfer (PET) reactions[8] have typically employed the electron acceptor methyl
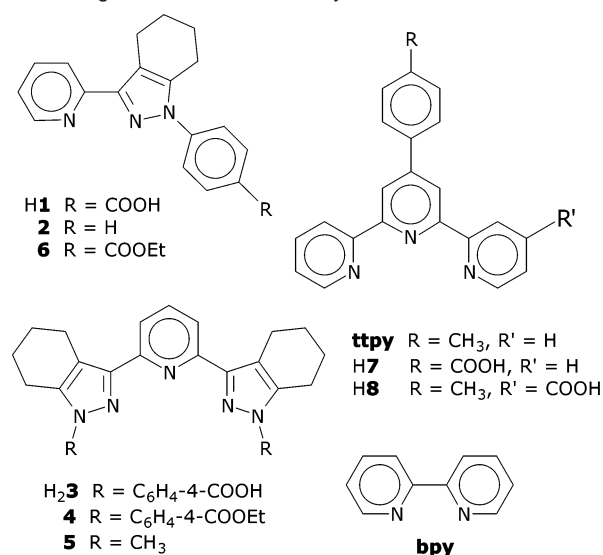
† On exchange from the University of Heidelberg.

(1) *Photogeneration of Hydrogen*; Harriman, A., West, M. A., Eds.; Academic Press: New York, 1983. *Photochemical Energy Conversion*; Norris, J. R., Meisel, D., Eds.; Elsevier: New York, 1989. Kalyanasundaram, K. *Photochemistry of Polypyridine and Porphyrin Complexes*; Academic Press: London, 1992. *Photosensitization and Photocatalysis using Inorganic and Organometallic Compounds*; Kalyanasundaram, K., Grätzel, M., Eds.; Kluwer Academic Press: Dordrecht, The Netherlands, 1993.

(2) Potvin, P. G.; Luyen, P. U.; Al-Mutlaq, F. *New J. Chem.* **2001**, *25*, 839.

(3) Mikel, C.; Potvin, P. G. *Polyhedron* **2002**, *21*, 49.

(4) Mikel, C.; Potvin, P. G. *Inorg. Chim. Acta* **2001**, *325*, 1.

(5) Vaduvescu, S.; Potvin, P. G. *Inorg. Chem.* **2002**, *41*, 4081.

(6) Kalyanasundaram, K. *Coord. Chem. Rev.* **1982**, *46*, 159.

(7) Constable, E. C. *Adv. Inorg. Chem. Radiochem.* **1986**, *30*, 69. Juris, A.; Balzani, V.; Barigelletti, F.; Campagna, S.; Belser, P.; von Zelewsky, A. *Coord. Chem. Rev.* **1988**, *84*, 85. Chan, S.; Wong, W.-T. *Coord. Chem. Rev.* **1995**, *138*, 219. Wong, W.-Y.; Wong, W.-T. *Coord. Chem. Rev.* **1995**, *146*, 307.

(8) Balzani, V.; Barigelletti, F.; De Cola, L. *Top. Curr. Chem.* **1993**, *159*, 1.

viologen (MV^{2+}), which also presents useful characteristics,[9] to produce an intermediate cation radical ($MV^{\bullet+}$) that can act as an electron relay in a photodriven redox reaction. The efficiency is limited in part by the lifetime of the photoexcited state (τ) which, in the case of $[Ru(bpy)_3]^{2+}$, is substantial (0.5–0.7 μs in H_2O,[6,10] 0.9–1.1 μs in CH_3CN[13]). It is also subject to electrostatic effects: not only does PET here involve an electrostatically unfavorable combination of cations, the reverse (or back) electron-transfer reaction (BET) between the Ru^{III} and $MV^{\bullet+}$ photoproducts, returning to starting materials, is actually *less* unfavorable. Our design solution is, first, to employ peripheral carboxyl groups to suppress electrostatic repulsions while, in most cases, leaving the core properties of the complex intact and, second, to use an organic solvent in order to help increase τ and enhance any electrostatic assistance that carboxylation provides. CH_3CN is a good choice, as it dissolves many Ru complexes, and is the solvent used in our sensitizer assessment protocol. PET has been studied with only a few carboxylated[15,16] or sulfonated Ru^{II} complexes and always in H_2O. Organo-solubility also addresses the second issue, photoproduct separation: if the PET reaction takes place at an organic–aqueous interface, the physical segregation of the photoproducts becomes possible, the benefits of which have been demonstrated with micelles and other heterogeneous microenvironments.[17] Ultimately, a three-phase system can be envisaged wherein an organo-soluble sensitizer embedded in a hydrophobic membrane mediates the electron transport between one aqueous phase hosting an oxidative half-reaction and the other supporting a reductive half-reaction.[18,19]

In this paper, we assess the effects of peripheral COO^- groups on PET to MV^{2+} in CH_3CN with a number of Ru^{II} complexes[20,21] made from bidentate[22] and tridentate[23] ligands (Chart 1), several of which have hydrophobic components for organo-solubility. We present evidence of significant supramolecular assistance of PET even with cationic sensitizers. The results are analyzed by reference to the operant electrostatic force fields, the supramolecular dissociation energies, and the activation energies for their electron-transfer reactions.

(9) Creutz, C.; Keller, A. D.; Sutin, N.; Zipp, A. P. *J. Am. Chem. Soc.* **1982**, *104*, 3618.
(10) Values reported include 0.69 μs (ref 11), 0.66 μs (Demas, J. N.; Adamson, A. W. *J. Am. Chem. Soc.* **1973**, *95*, 5159), 0.60 μs (Lin, C.-T.; Boettcher, W.; Chou, M.; Creutz, C.; Sutin, N. *J. Am. Chem. Soc.* **1976**, *98*, 6536), 0.59 μs (ref 12 and Sriram, S.; Hoffman, M. Z. *Chem. Phys. Lett.* **1982**, *85*, 572), 0.58 μs (Van Houten, J.; Watts, R. W. *J. Am. Chem. Soc.* **1976**, *98*, 4853), 0.50 μs (Rodgers, M. A. J.; Becker, J. C. *J. Phys. Chem.* **1980**, *84*, 2762).
(11) Keller, P.; Moradpour, A.; Amouyal, E.; Kagan, H. B. *Nouv. J. Chim.* **1980**, *4*, 377.
(12) Chu, D. Y.; Thomas, J. K. *J. Phys. Chem.* **1985**, *89*, 4065.
(13) Values reported include 0.85 μs (ref 14) and 1.1 μs (Bensasson, R. V.; Salet, C.; Balzani, V. *J. Am. Chem. Soc.* **1976**, *98*, 3722).
(14) DeLaive, P. J.; Lee, J. T.; Sprintschnik, H. W.; Abruna, H.; Meyer, T. J.; Whitten, D. G. *J. Am. Chem. Soc.* **1977**, *99*, 7094.
(15) Gaines, G. L. *J. Phys. Chem.* **1979**, *83*, 3088.
(16) Anderson, S.; Constable, E. C.; Seddon, K. R.; Turp, J. E.; Baggott, J. E.; Pilling, M. J. *J. Chem. Soc., Dalton Trans.* **1985**, 2247.
(17) Kalyanasundaran, K. *Photochemistry in Microheterogeneous Systems*; Academic Press: New York, 1987. Grätzel. M. *Heterogeneous Photochemical Electron Transfer*; CRC Press: Boca Raton, FL, 1989. *Molecular and Supramolecular Photochemistry*; Ramamurthy, V., Schanze, K. S., Eds.; Marcel-Dekker: New York, 1997; Vol. 1.
(18) Sutin, N.; Creutz, C. *Pure Appl. Chem.* **1980**, *52*, 2717.
(19) Lymar, S. V.; Parmon, V. N.; Zamarev, K. I. *Top. Curr. Chem.* **1991**, *159*, 1.
(20) Luo, Y.; Potvin, P. G.; Tse, Y.-H.; Lever, A. B. P. *Inorg. Chem.* **1996**, *35*, 5445.
(21) Zadykowicz, J.; Potvin, P. G. *Inorg. Chem.* **1999**, *38*, 2434.
(22) Luo, Y.; Potvin, P. G. *J. Org. Chem.* **1994**, *59*, 1761.
(23) van der Valk, P.; Potvin, P. G. *J. Org. Chem.* **1994**, *59*, 1766. Zadykowicz, J.; Potvin, P. G. *J. Org. Chem.* **1998**, *63*, 235.

Chart 1. Ligands Used in This Study

2. Experimental Section

Ru(bpy)$_3$Cl$_2$ was a commercial material that was used as received. The $[Ru(\mathbf{6})_2(bpy)](PF_6)_2$ used was the symmetric isomer with trans indazole groups (labeled β in ref 20).

2.1. [Ru(Na1)$_2$(bpy)](PF$_6$)$_2$.[24] $[Ru(\mathbf{6})_2(bpy)](PF_6)_2$ (0.21 g, 0.17 mmol) was heated overnight under reflux in 6 mL of 0.1 M NaOH and 20 mL of H_2O. After vacuum-drying of the reaction mixture, the residue was extracted into CH_3CN and filtered free of insoluble materials. The filtrate was evaporated to provide 0.19 g (91%) of an orange powder. An analytical sample was prepared by crystallization from MeOH/Et$_2$O.

2.2. [Ru(H7)(ttpy)](PF$_6$)$_2$ and [Ru(H7)$_2$](PF$_6$)$_2$. Following a general procedure of Cullis and Ladbury,[25] we dissolved $[Ru(ttpy)_2]Cl_2$ (70 mg, 8.6×10^{-5} mol) in 25 mL of H_2O and then heated the mixture to 100 °C, followed by the slow addition of KMnO$_4$ (108 mg, 8 equiv) dissolved in 5 mL of H_2O over 6 h. The reaction mixture was cooled to room temperature after 53 h, rid of solvent, then purified by column chromatography (75 g SiO$_2$, 14:2:1 CH_3CN/saturated KNO$_{3(aq)}$/H_2O, h = 15 cm, ϕ = 6 cm). The less polar product was identified as the singly oxidized $[Ru(H\mathbf{7})(ttpy)](NO_3)_2$. This was transformed to the PF_6^- salt by precipitation from CH_3OH with excess aqueous NH$_4$PF$_6$ (yield 22 mg, 24%). The more polar product was the doubly oxidized $[Ru(H\mathbf{7})_2](NO_3)_2$. It was poorly soluble in CH_3OH and was therefore dissolved in a weakly basic (KOH) CH_3OH/H_2O mixture, to which was added a saturated aqueous NH$_4$PF$_6$ solution containing dilute nitric acid (pH = 7). Precipitation occurred upon evaporation. This was redissolved in CH_3CN and reprecipitated with aqueous NH$_4$PF$_6$, and this process was repeated twice more to minimize contamination by nitrate salts. Yield 22 mg (24%).

2.3. Photochemical Measurements. This used the apparatus, sample preparation, and data treatment previously described.[2] Each sample contained 4×10^{-5} M sensitizers as PF_6^- salts, 9.45×10^{-5} M MV-(PF$_6$)$_2$, and 0.05 M TEOA in CH_3CN. They were stirred and maintained at 25 °C. Except where noted in Table 1, three samples were used for each sensitizer, and each sample was taken through three cycles of growth (under continuous irradiation over the 400–600 nm range) and decay (in the dark), providing three sets of data used to determine the rate constants of eq 1 as weighted averages computed, along with experimental uncertainties, by standard means.[2]

2.4. Computations. The Supporting Information gives the general expression for the electrostatic force F felt by guests (MV^{2+}, $MV^{\bullet+}$, or

(24) Luo, Y. Ph.D. Thesis, York University, 1993.
(25) Cullis, J. D.; Ladbury, C. W. *J. Chem. Soc.* **1955**, 555.

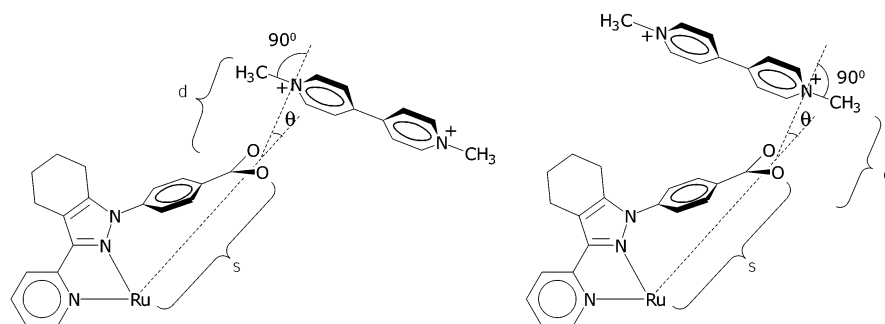**Figure 1.** Two possible orientations of a MV^{2+} or MV$^{•+}$ guest relative to an Ru···COO$^-$ axis for a given angle θ, with quantities d, s, and θ defined.

Table 1. Uncertainty-Weighted Averages[a] in MV$^{•+}$ Yields and in Rate Constants from CH$_3$CN Solutions

complex	χ^{obs} /%	k_{init} /10^{-5} s^{-1}	k_f /10^{-5} s^{-1}	k_q /10^{-3} s^{-1}	χ^{theor} /%
[Ru(H**1**)(bpy)$_2$]$^{2+}$	0.39(1), 0.22(5)[b,c]	30.9(3), 4.1(2)[b]	37.1(5)	35(4)	1.1(1)
[Ru(bpy)$_3$]$^{2+}$	0.38(3), 0.66(1)[b,d]	26.5(7), 11.0(2)[b]	30.2(5)	30.6(4)	0.98(2)
[Ru(H**1**)$_2$(bpy)]$^{2+}$	0.15(3), 0[b,e]	3.18(9)	3.35(4)	5.3(6)	0.63(7)
[Ru(H**8**)$_2$]$^{2+f}$	0.14(2)	1.72(4)	1.86(3)	5.9(18)	0.31(9)
[Ru(H**7**)$_2$]$^{2+}$	0.093(1)	1.77(5)	1.81(5)	7.89(5)	0.23(1)
[Ru(H**7**)(ttpy)]$^{2+}$	0.12(1)	1.31(5)	1.596(2)	6.1(5)	0.26(2)
[Ru(ttpy)$_2$]$^{2+}$	0.059(5)	0.84(1)	1.12(1)	8.8(6)	0.13(1)
[Ru(H$_2$**3**)$_2$]$^{2+}$	0.053(2), 0[b,e]	0.506(7)	0.54(3)	4.4(13)	0.12(4)
[Ru(H**1**)$_3$]$^{2+g}$	0.040(3)	0.24(1)	0.44(4)	4.4(9)	0.10(2)
[Ru(**5**)$_2$]$^{2+h}$	0.030(7)	0.32(9)	0.31(1)	0.8(7)	*i*
[Ru(**4**)$_2$]$^{2+h}$	0.028(5)	0.20(4)	0.20(2)	0.19(12)	*i*
[Ru(**2**)$_3$]$^{2+h}$	0.026(5)	0.16(2)	0.16(5)	0.28(18)	*i*

[a] In brackets are the experimental uncertainties in the least significant digits. [b] In H$_2$O. [c] Total yield 0.90(5)%. [d] Four samples. Total yields 3.8(0)% in H$_2$O and 2.3(3)% in 80% CH$_3$CN. [e] In 80% CH$_3$CN. [f] Data from ref 3. [g] Two cycles per sample. [h] One sample. [i] Uncertainty too large to provide a meaningful value.

HTEOA$^+$, or combinations thereof) near a mono- or dicarboxylated Ru^{II} or Ru^{III} host complex as well as an expression for the corresponding dissociation energies E, obtained by integration of F over the approach distance d (Figure 1). With dicarboxylated hosts, various orientations of MV^{2+}/MV$^{•+}$ guests are available. All were assessed, and the most stable orientation in each host−guest pair was retained.

For these computations, we used estimates of s (defined in Figure 1) and r, the COO$^-$···COO$^-$ separation in dicarboxylated cases, given in Tables 2 and 3. For [Ru^{II}(**1**)(bpy)$_2$]$^+$ and [Ru^{II}(**1**)$_2$(bpy)]^0, average values of these parameters were calculated from the crystal structure of the diester [Ru(**6**)$_2$(bpy)]$^{2+}$.[20] No crystallographic estimates were available for the other carboxylated complexes. For [Ru(H$_2$**3**)(H**3**)]$^+$ and [Ru(H$_2$**3**)(**3**)]^0, we used the average N(2)···COO$^-$ distance from crystalline [Ru(**6**)$_2$(bpy)]$^{2+}$ plotted along the N^2−CH$_3$ bond vector in the crystal structure[31] of the 1,1″-dimethyl analogue [Ru(**5**)$_2$]$^{2+}$. For [Ru(H**8**)(**8**)]$^+$ and [Ru(**8**)$_2$]^0,[3] a similar procedure used the average N(1)···COO$^-$ separation measured from the crystal structure of Ru-(H$_2$dcbpy)$_2$(SCN)$_2$[26] (H$_2$dcbpy is 2,2′-bipyridine-4,4′-dicarboxylic acid) applied to the N(1)−C4 vector of [Ru(tpy)$_2$](ClO$_4$)$_2$[27] (tpy is 2,2′:6′,2″-terpyridine). The former crystal structure also provided estimates of r (7.43 Å) and s (6.33 Å) for [Ru(dcbpy)(bpy)$_2$]^0. For [Ru(**7**)(ttpy)]$^+$ or [Ru(H**7**)(**7**)]$^+$ and [Ru(**7**)$_2$]^0, the average Ru···CH$_3$ distances in two crystal structures containing the ttpy ligand[4,28] were used to estimate an average s, and r for [Ru(**7**)$_2$]^0 is twice that value. The N$^+$···N$^+$ separation l in MV^{2+} was taken as 7.00 Å from the crystal structure of the dibromide salt.[29] For all guests, a common approach distance d of 2.9 Å was adopted as a reasonable estimate of the O$^-$···N$^+$ van der Waals distance and the O$^-$···H−N$^+$ hydrogen bonding distance.[30] While

keeping the N···N axes of MV^{2+}/MV$^{•+}$ orthogonal to the COO$^-$···N vector(s), the θ angles were adjusted to maximize F.

Isodynamic contour diagrams representing the fields felt by a single positive charge (Figure 4) were constructed as x,y plots by, first, aligning the Ru···COO$^-$ vectors of monocarboxylated sensitizers along the positive y axis with Ru at the origin and then setting $d^2 = (y − s)^2 + x^2$ and solving for x at various values of F and y. In general, for a monocarboxylated complex whose metal charge is q_M, F will be attractive (>0) within a sphere of radius $sq_M^{1/2}/(q_M − 1)$ centered at an outward distance $s/(q_M − 1)$ from the COO$^-$ group and reaching to a distance $s(q_M^{1/2} + 1)/(q_M − 1)$ along the Ru−COO$^-$ vector. For dicarboxylated cases, the x axis was set as bisecting the two Ru−COO$^-$ vectors, and the electrostatic boundaries of Figure 5 were similarly determined at $F = 0$. Minimum bubble sizes are those required for monocarboxylated hosts to accommodate MV^{2+}/MV$^{•+}$ guests; they were calculated as the maximum s value satisfying $F \leq 0$. With Ru^{II}, s needs to be ≥ 1.414 Å to accommodate MV^{2+} (at optimal tilt angle $\theta = 81°$). For MV$^{•+}$ and Ru^{III}, $s \geq 2.567$ Å with optimal $\theta = 76°$.

3. Results

3.1. Synthesis. All but three complexes used in this study (Table 1) have been previously reported.[3,20,21,31] [Ru(H**7**)(ttpy)]-(PF$_6$)$_2$ and [Ru(H**7**)$_2$](PF$_6$)$_2$ were obtained together, in 24% isolated yields each, by KMnO$_4$ oxidation of [Ru(ttpy)$_2$]Cl$_2$. To our knowledge, this constitutes the first side-chain oxidation of a Ru complex. These acidic complexes remained homogeneous in the dilute solutions used in UV−visible spectrometry and in the photochemical experiments, but in concentrated CH$_3$CN solutions appropriate for crystallization, they tended to form CH$_3$CN-insoluble precipitates. Moreover, the evaporation of their solutions and redissolution left insoluble residues. These insoluble materials could be solubilized in the presence of a small amount of TFA, and we believe they resulted from the

(26) Shklover, V.; Ovchinnikov, Yu. E.; Braginsky, L. S.; Zakeeruddin, S. M.; Grätzel, M. *Chem. Mater.* **1998**, *10*, 2533.
(27) Craig, D. C.; Scudder, M. L.; McHale, W.-A.; Goodwin, H. A. *Aust. J. Chem.* **1998**, *51*, 1131.
(28) Chamchoumis, C. M.; Potvin, P. G. *J. Chem. Soc., Dalton Trans.* **1999**, 1373.
(29) Russell, J. H.; Wallwork, S. C. *Acta Crystallogr.* **1972**, *B28*, 1527.
(30) Jeffrey, G. A.; Maluszynska, H. *Int. J. Biol. Macromol.* **1982**, *4*, 173.

loss of the elements of HPF$_6$, as had occurred with previous carboxyl-bearing Ru^{II} complex PF$_6^-$ salts, including [Ru(H$_2$3)$_2$]-(PF$_6$)$_2$.[21] Difficulties in handling acidic PF$_6^-$ salts have also been noted by others.[32] Probably because of this difficulty, no satisfactory elemental analyses were obtained, but the samples were chromatographically homogeneous and their NMR spectra (Supporting Information) were free of extraneous signals. Other than Cl$^-$, whose salts are too insoluble in organic solvents, other counteranions have not been explored. The Na$^+$ salts of these complexes were too poorly soluble in CH$_3$CN to be useable.

The stable compound [Ru(Na1)$_2$(bpy)](PF$_6$)$_2$ was obtained in 91% yield by saponification of the corresponding diester complex without acidification. Its formulation as an adduct of NaPF$_6$ was confirmed by elemental analysis. In this case, the fused cyclohexane rings evidently conferred sufficient solubility in CH$_3$CN.

3.2. Photogeneration of MV^{2+}. Samples of the sensitizers were prepared and treated as detailed earlier.[2] This involved the continuous irradiation at 400–600 nm of stirred solutions containing the sensitizer and excesses of MV^{2+} and of TEOA, as sacrificial reductant, at uniform concentrations and at 25 °C for all examples. The results were consistent, within experimental error, over time and from day to day, so that any variations in light intensity were deemed small. The concentrations of MV$^{\bullet+}$ were spectrophotometrically monitored over time during irradiation and during its decay in the dark. Typical time courses for the MV$^{\bullet+}$ absorbance at 600 nm (A_t) are presented in Figure 2 for representative examples. In CH$_3$CN, there is slow to rapid growth in A_t under visible-light irradiation that slopes off to reach a "steady-state" plateau region. When the irradiation is stopped, the absorbance decays back to the starting point, owing to aerobic quenching of MV$^{\bullet+}$ (Scheme 1, reaction 4).

The maximal A_t values were converted to observed yields of MV$^{\bullet+}$ (χ^{obs}). The initial A_t growth rates were assessed as the least-squares slopes of A_t over the first sixth or seventh of the growth phase (5–40 s) and then converted to a first-order rate constant (k_{init} = rate/[MV^{2+}]$_0$) for comparison purposes. The A_t data were converted to [MV$^{\bullet+}$]$_t$ values, which were then fitted to the kinetic model developed earlier.[2]

$$\mathrm{d[MV^{\bullet+}]}_t/\mathrm{d}t = k_f[\mathrm{MV^{2+}}]_0 - (k_f + k_q + k_{d1})[\mathrm{MV^{\bullet+}}]_t - k_{d2}[\mathrm{MV^{\bullet+}}]_t^2 \quad (1)$$

where k_f is the *pseudo*-first-order rate constant for the photosensitized formation of MV$^{\bullet+}$ via oxidative quenching of the Ru^{II} excited state by MV^{2+} (Scheme 1, reaction 1), k_q is the *pseudo*-first-order rate constant for the reverse quenching of MV$^{\bullet+}$ by the Ru^{III} photoproduct (Scheme 1, reaction 5), k_{d2} is the *pseudo*-second-order rate constant for the quenching of MV$^{\bullet+}$ by O$_2$ (Scheme 1, reaction 4), and k_{d1} is the corresponding first-order contribution. The values of k_{d1} and k_{d2} were first determined by a nonlinear fit of the data from the subsequent second-order decay of A_t in the dark, where quenching is by O$_2$ alone, using eq 1 with k_f and k_q set to 0. The k_{d1} term was usually negligible. Mechanistic grounds for eq 1 were presented earlier.[2] We also computed the MV$^{\bullet+}$ yield theoretically
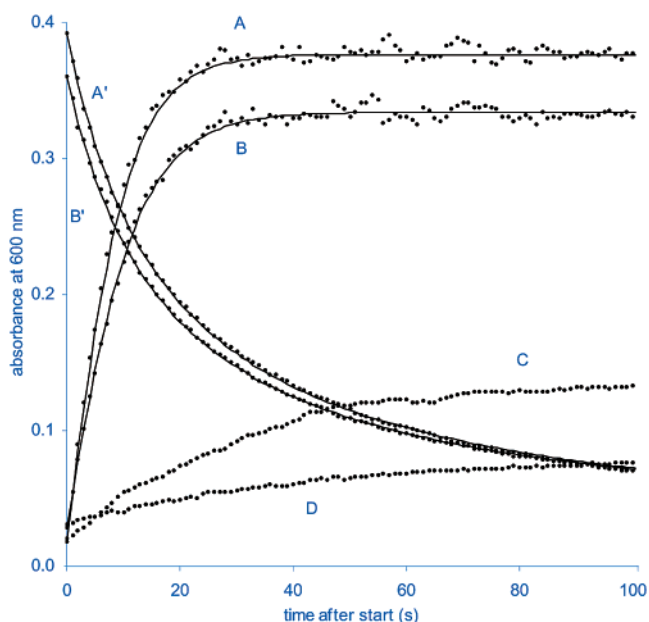
(31) Zadykowicz, J.; Potvin, P. G. *J. Coord. Chem.* **1999**, *47*, 395.
(32) Hammarström, L.; Alsins, J.; Börje, A.; Norrby, T.; Zhang, L.; Ckermark, B. *J. Photochem. Photobiol.* **1997**, *A102*, 139.

Figure 2. Typical evolution of absorbance at 600 nm using [Ru(bpy)$_2$-(H1)]$^{2+}$ under irradiation (A) and, afterward, in the dark (A′), in 4 × 10^{-5} M CH$_3$CN solution. The corresponding plots with [Ru(bpy)$_3$]$^{2+}$ are labeled B and B′, respectively. Plots C and D were obtained with [Ru(bpy)(H1)$_2$]$^{2+}$ and [Ru(ttpy)$_2$]$^{2+}$, respectively. The solid lines are the fitted curves.

Scheme 1. Reactions Involved in MV$^{\bullet+}$ Production Using the Sacrificial Reductant TEOA^a
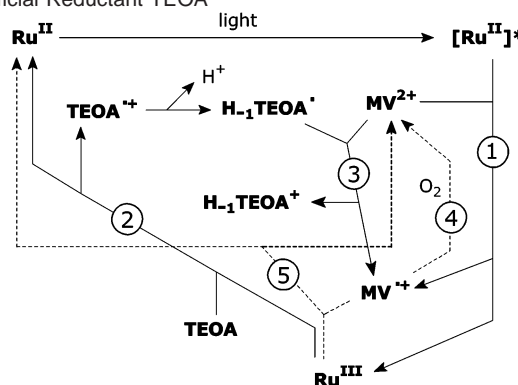
^{a} Solid lines indicate productive reactions: (1) PET, (2) sacrificial reduction, (3) secondary generation, suppressed by O$_2$. Reactions with dashed lines are counterproductive: (4) aerobic quenching, (5) reverse or back electron transfer (BET).

achievable in an O$_2$-free system ($k_{d1} = k_{d2} = 0$), given by

$$\chi^{theor} = [\mathrm{MV^{\bullet+}}]_\infty^{theor}/[\mathrm{MV^{2+}}]_0 = k_f/(k_f + k_q)$$

Overall, a better sensitizer will be indicated by higher k_f and χ^{theor} values. Of these, k_f is more reliably measured than χ^{theor}, owing to a greater variability in k_q, and spans a broader range of values. The k_{init} values, although they consistently underestimate k_f by about 15%, nevertheless show an excellent correlation with it ($r > 0.999$). Because of the vagaries of O$_2$ content, a higher χ^{obs} value does not necessarily indicate a better sensitizer. A case in point is Ru(H1)(bpy)$_2$$^{2+}$, which, although it is indistinguishable within experimental error from Ru(bpy)$_3$$^{2+}$ in terms of χ^{obs}, shows distinctly better kinetic parameters. Another case is [Ru(H8)$_2$](PF$_6$)$_2$, which shows a net higher χ^{obs} than that of [Ru(H7)$_2$](PF$_6$)$_2$, but the differences in their kinetic parameters are not statistically significant. A higher k_f also leads
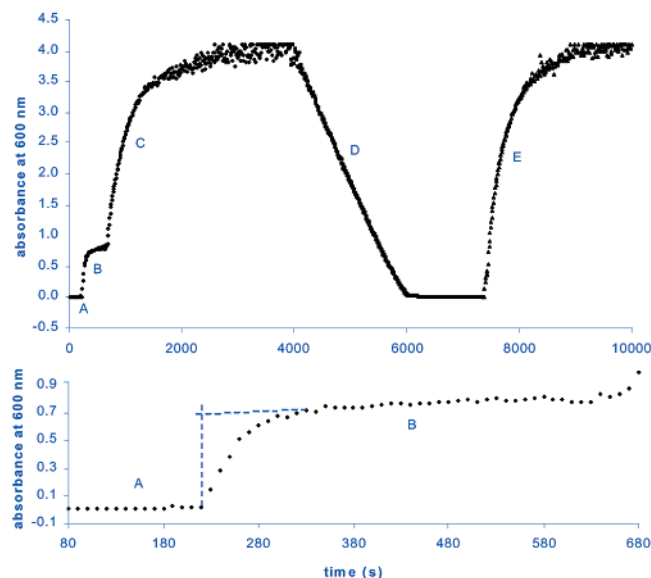
Figure 3. Plots of A_t vs time using Ru(bpy)$_3$Cl$_2$ in H$_2$O (upper plot) and the extrapolation used to measure TEOA-independent yields (lower trace).

to a higher k_q because faster MV$^{•+}$ formation leads to more Ru^{III} and therefore to a faster reaction 5 in Scheme 1.

Some samples were also assessed in H$_2$O or 4:1 CH$_3$CN–H$_2$O for comparison. An illustrative time course with Ru(bpy)$_3$$^{2+}$ in H$_2$O is presented as Figure 3. As detailed earlier,[2] sensitizer assessments in aqueous solvents are not as useful. Only the good sensitizers Ru(bpy)$_3$$^{2+}$ and Ru(H**1**)(bpy)$_2$$^{2+}$ generated any MV$^{•+}$ in these solvents, but, more importantly, the MV$^{•+}$ evolution was much slower and more complicated, due to a secondary production of MV$^{•+}$ by the deprotonated and oxidized form of the sacrificial reductant, H$_{-1}$TEOA$^{•}$ (Scheme 1, reaction 3).[33,34] This is initially suppressed by O$_2$, which furthermore efficiently quenches MV$^{•+}$ in aqueous media, resulting in a variable period of induction (part A in Figure 3) while the sample is undergoing a depletion of O$_2$. This is followed by the onset of TEOA-independent growth (part B), overtaken by TEOA-dependent growth (part C) that brings the absorbance to detector saturation. The intervening dark decay portions (part D) were slower than those in CH$_3$CN and zeroth-order in [MV$^{•+}$] and, hence, diffusion-limited. Subsequent irradiations (part E) were O$_2$-poor throughout, that is, without induction, and the two channels of MV$^{•+}$ generation overlapped. Since the instantaneous k_{d2} was not constant (and unknown) during the first growth (part B), eq 1 could not be applied, but we noted that the MV$^{•+}$ yield during this phase was fairly constant from sample to sample. To measure these yields independent of the TEOA-related growth, we extrapolated the slow-rising plateau of region B back to the start of the first growth. These estimates must be interpreted with the appropriate caution. The initial rate constants (k_{init}) were also assessed over the first 40 s of growth during phase B and averaged over three samples.

Samples run in 4:1 CH$_3$CN–H$_2$O behaved similarly but suffered longer induction periods (A) and lacked any detectable first growth phase (B), so that only the total MV$^{•+}$ yield could be measured.

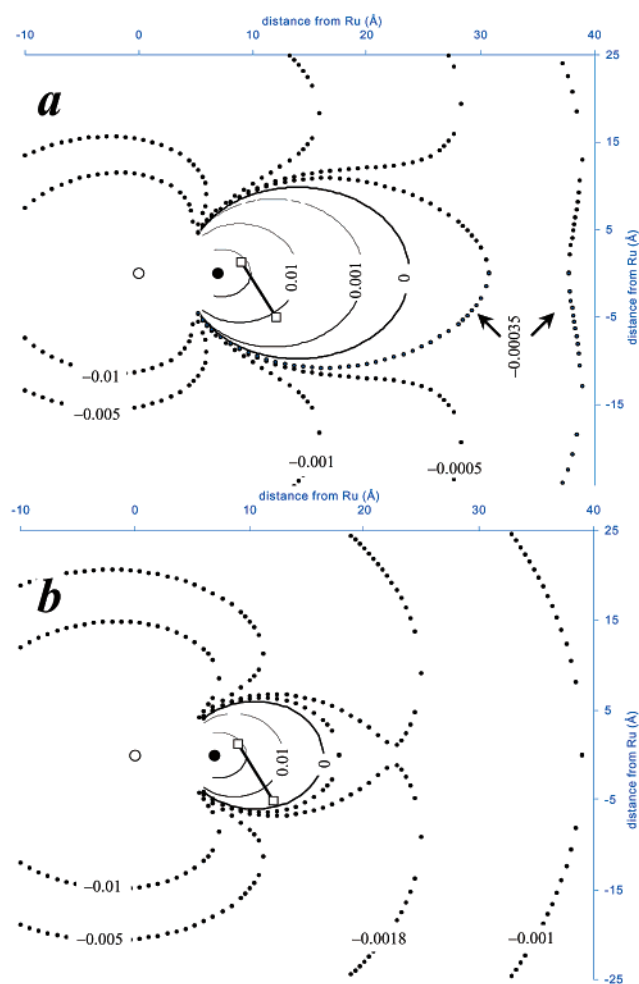**3.3. Computations.** We suspected that the benefits of carboxylation on photoactivity evident from Table 1 were a

(33) Neshvad, G.; Hoffman, M. Z. *J. Phys. Chem.* **1989**, *93*, 2445.
(34) Kalyanasundaram, K.; Kiwi, J.; Grätzel, M. *Helv. Chim. Acta* **1978**, *61*, 2720.

Figure 4. Isodynamic contours of the electrostatic fields felt by a monocation in the vicinity of [Ru$^{II/III}$(**1**)(bpy)$_2$]$^{+/2+}$ ($s = 6.94$ Å): (a) before PET or (b) after PET. The Ru location is indicated by the unfilled circle, while that of the COO$^-$ group is given by the filled circle. Solid lines indicate attraction; dotted lines indicate repulsion. The forces are given for each line in multiples of $e^2/(4\pi\rho\epsilon_0)$. The fields are symmetrical about the Ru⋯COO$^-$ axes. The optimal positioning of MV^{2+} is indicated by the line joining the unfilled squares that mark the N$^+$ centers.

result of useful electrostatic interactions between MV^{2+} and the peripheral COOH groups in ionized form within an otherwise repulsive environment. To substantiate this, we wished to compute the free energies of activation for electron transfer (ΔG^*) from the classical Marcus theory of electron-transfer kinetics.[35] According to this theory, ΔG^* is related to the free energy of reaction (ΔG°), the total reorganizational energy (here denoted by Λ instead of the usual λ, to differentiate it from wavelengths), and the work terms required to achieve product (W_P) and reactant (W_R) states (corresponding to the work required to bring the products or reactants together in a bimolecular scenario to a given mean separation distance):

$$\Delta G^* = W_R + (\Delta G^\circ + \Lambda + W_P - W_R)^2/4\Lambda \qquad (2)$$

With experimental values of the redox potentials and emission λ_{max}, one can estimate the driving force ΔG° for PET by using the Rehm–Weller equation[36]

(35) Marcus, R. A.; Sutin, N. *Biochim. Biophys. Acta* **1985**, *811*, 265.
(36) Rehm, D.; Weller, A. *Ber. Bunsen-Ges. Phys. Chem.* **1969**, *73*, 834.

Table 2. Dissociation Energies E (kJ mol^{-1}) of Substrates from Singly Carboxylated Complexes of Ru$^{II/III}$ and Ligands L, s (Å) and Tilt Angles θ (deg) for MV^{2+}/MV$^{\bullet+}$

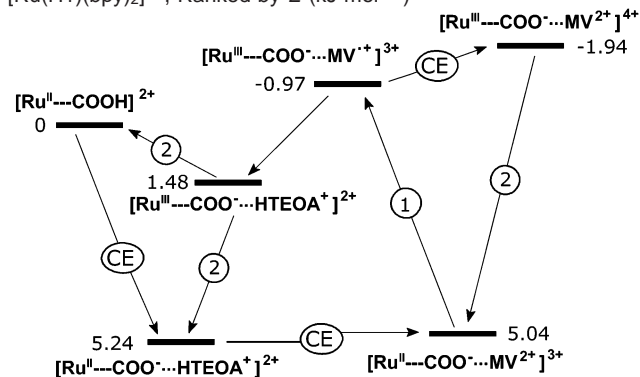| L	8$^-$		H3$^-$		1$^-$		7$^-$	
s (Å)	6.36		6.87		6.94		10.55	
θ (deg)	64.1		64.1		64.0		58.8	
oxidn state	II	III	II	III	II	III	II	III
MV^{2+} ^{a}	4.26	-3.10	4.94	-2.07	5.04	-1.94	8.37	3.07
HTEOA$^+$	4.77	0.77	5.18	1.39	5.24	1.48	7.26	4.51

^{a} Values for MV$^{\bullet+}$ will be half those for MV^{2+}.

$$\Delta G^{\circ}{}_{\text{PET}} = E_{\text{ox}}(\text{Ru}^{\text{III/II}}) - E_{\text{red}}(\text{MV}^{2+/\bullet+}) - E_{00} \qquad (3)$$

Dropping the E_{00} term provides an estimate of $-\Delta G^{\circ}$ for BET. The Λ values can be estimated by standard means after assuming, as is true with [Ru(bpy)$_3$]$^{2+}$, that the inner-sphere component is negligible.[35]

In the present situation, the work terms W are mainly electrostatic; they are small in polar solvents and frequently omitted for "notational brevity"[37] but are significant in less polar solvents. Except at long range, these interactions cannot be adequately described nor quantified using the simple point-charge models usually applied. Instead, we defined the Coulombic force fields near the carboxylated hosts by summing the attractions and repulsions present at points in the surrounding space, with knowledge of the Ru$\cdots$COO$^-$ separation(s), and, for the dicarboxylated cases, the COO$^-\cdots$COO$^-$ separations and COO$^-\cdots$Ru$\cdots$COO$^-$ angles. We found the best orientations of guests MV^{2+}/MV$^{\bullet+}$ and/or HTEOA$^+$ near the carboxylated hosts as those which maximized the net Coulombic forces F and then calculated the energies E required to remove the guest(s) to infinity.

Figure 4 depicts the isodynamic contour lines of the electrostatic force field F felt by a monocation near [Ru$^{II/III}$(**1**)(bpy)$_2$]$^{+/2+}$. The presence of a COO$^-$ group defines a sphere or "bubble" of space that is attractive to cations within the larger, repulsive space. This particular bubble has a diameter of 19.6 Å and extends 16.8 Å away from the COO$^-$ group and is thus large enough to comfortably accommodate MV^{2+} or even the cationic sensitizers themselves. The total force felt by the dication MV^{2+} will depend on its orientation relative to the Ru$\cdots$COO$^-$ axis, and since the nitrogens are independent of one another, the net force will be the sum of the forces felt by each. The numbers of Figure 4 well approximate an end-on orientation, wherein the second, distal nitrogen contributes negligibly. An end-on approach is optimal at medium and long ranges, and the approach of least repulsion and maximal attraction is along the Ru$\cdots$COO$^-$ axis. Within the bubble, the optimal orientation of MV^{2+} is calculated to be at a tilt of $\theta = 64°$ from the Ru$\cdots$COO$^-$ axis at van der Waals contact distance. As a result of PET, the metal becomes more repulsive and the attractive terms weaken. The attractive bubble will then have a reduced diameter of 12.0 Å and will extend only 9.5 Å beyond the COO$^-$ group. The optimal orientation of MV^{2+}/MV$^{\bullet+}$ remains the same. Analogous bubbles result with [Ru(H$_2$**3**)(H**3**)]$^+$, [Ru(H**7**)(**7**)]$^+$ or [Ru(**7**)(ttpy)]$^+$, and [Ru(H**8**)(**8**)]$^+$, the size of which is linearly dependent on s, the metal–carboxyl distance. The optimal orientation of HTEOA$^+$ has $\theta = 0°$ in all cases.

(37) Marcus, R. A. Nobel Prize Lecture, 1992.

Scheme 2. Species Involved in Productive Reactions 1 and 2 (from Scheme 1) via Cation Exchange Steps (Marked CE), with [Ru(H1)(bpy)$_2$]$^{2+}$, Ranked by E (kJ mol^{-1})

The dissociation energy E for each host–guest combination at nearest approach and at the optimal θ values is reported in Table 2. Scheme 2 is the corresponding energy level diagram for [Ru$^{II/III}$(**1**)(bpy)$_2$]$^{+/2+}$. The other cases lead to entirely similar diagrams (Supporting Information). The sensitivity of these results to the value of d was tested (Supporting Information). The E values were only slightly sensitive (up to 0.4 kJ mol^{-1} change per 0.1 Å variation in d) and changed in unison, so that their relative ordering in Scheme 2 was robust. Further, the selectivity for pre-PET versus post-PET binding, expressed as $E(\text{Ru}^{II}/\text{MV}^{2+}) - E(\text{Ru}^{III}/\text{MV}^{\bullet+})$, was even less sensitive.

Scheme 2 reveals that cation exchange is a means of effecting the post-PET dissociation of MV$^{\bullet+}$ from Ru^{III} at low energetic cost. The driving force for the exchange of any guest for another is the difference between their respective dissociation energies. Table 2 reveals that the exchange of MV$^{\bullet+}$ by HTEOA$^+$ is always favorable after PET (i.e., with Ru^{III}). Only with ligand **7**$^-$ is the exchange of MV$^{\bullet+}$ by MV^{2+} also favorable. This is because $E < 0$ for MV^{2+}/MV$^{\bullet+}$ with all ligands except **7**$^-$, even if $F > 0$. E becomes negative when the dissociation of the distal nitrogen in MV^{2+}/MV$^{\bullet+}$ is sufficiently exergonic after PET as to balance or outweigh the endergonic dissociation of the proximal nitrogen, as occurs whenever $s < 8.11$ Å, as with all cases except **7**$^-$.

Charge delocalization was assumed for MV$^{\bullet+}$ in these computations. If the charge is actually localized (at the extreme, one nitrogen is neutral), then MV$^{\bullet+}$ emulates HTEOA$^+$ in that the E values will be less negative or more positive, with the result that the driving forces for the exchanges of charge-localized MV$^{\bullet+}$ after PET become less favorable, as with HTEOA$^+$, or more unfavorable, as with MV^{2+}.

To place these E values in perspective, we can estimate the corresponding values for the dissociation of [Ru(bpy)$_3$]$^{2+/3+}$ from MV$^{2+/\bullet+}$ (ionic radii $R_A = 7.0$ Å and $R_B = 3.3$ Å, respectively)[38] from within contact distance ($R_A + R_B$) in CH$_3$-CN (dielectric constant $\rho = 37.5$), using the simple formula[39]

$$E = -q_A q_B e^2 / 4\pi\epsilon_0 \rho (R_A + R_B)$$

which neglects ionic strength effects ($\mu = 0.028$ M in these experiments). This gives -14.4 kJ mol^{-1} before PET and -10.8 kJ mol^{-1} after PET. The corresponding values for the *un-ionized*

(38) Sun, H.; Yoshimura, A.; Hoffman, M. Z. *J. Phys. Chem.* **1994**, *98*, 5058.
(39) Tkachenko, N. V.; Tauber, A. Y.; Grandell, D.; Hynninen, P. H.; Lemmetyinen, H. *J. Phys. Chem. A* **1999**, *103*, 3646.

Figure 5. Limits of the attractive regions surrounding dicarboxylated complexes [Ru(**7**)₂]⁰ (a), [Ru(H₂**3**)(**3**)]⁰ (b), and [Ru(**1**)₂(bpy)]⁰ (c), using common *x* and *z* scales. The solid isodynamic lines delimiting large sectors pertain to Ru^II before PET, and the dotted enclosed surfaces, to Ru^III after PET. The metal positions are given by white spheres at the origins. The optimal locations of MV²⁺/MV•⁺ before PET are indicated by the solid bars.

[Ru(H**1**)(bpy)₂]²⁺/³⁺ were calculated with $R_A = s + 2.9/2$ Å, where 2.9 Å represents the approach distance used throughout, at −12.7 kJ mol⁻¹ for [Ru^II(H**1**)(bpy)₂]²⁺ with MV²⁺ and −9.5 kJ mol⁻¹ for [Ru^III(H**1**)(bpy)₂]³⁺ with MV•⁺, values too high to include in Scheme 2. Ionization then apparently affords a stabilization of nearly 18 kJ mol⁻¹ pre-PET and nearly 11 kJ mol⁻¹ post-PET. Similarly large values occur with the other carboxylated cases.

To estimate association equilibrium constants for comparative purposes, the formula used by Kavarnos[40] and Sutin[35]

$$K_{assoc} = 4\pi(R_A + R_B)^2 \delta e^{-W_R/RT}$$

was employed, where δ represents the thickness of the shell within which PET can occur and is taken to be 0.8 Å.[35] Using the same R_A values as before, the preassociation is mildly favorable, as K_{assoc} at 298 K is 6.3 M⁻¹ for [Ru^II(**1**)(bpy)₂]⁺ with MV²⁺ (cf. 6.9 M⁻¹ with HTEOA⁺), and becomes mildly unfavorable after PET, as K_{assoc} falls to 0.56 M⁻¹ for [Ru^III(**1**)-(bpy)₂]²⁺ with MV•⁺ (cf. 1.5 M⁻¹ with HTEOA⁺ and 0.38 M⁻¹ with fresh MV²⁺). In contrast, the association of [Ru^II(bpy)₃]²⁺ with MV²⁺ is highly unfavorable ($K_{assoc} = 1.9 \times 10^{-3}$ M⁻¹) but becomes less so after PET ($K_{assoc} = 8.3 \times 10^{-3}$ M⁻¹).

We can estimate equilibrium constants K_{eq} for the exchange of one guest (G₁) for another (G₂) by host H:

$$H\cdots G_1 + G_2 \underset{}{\overset{K_{eq}}{\rightleftharpoons}} H\cdots G_2 + G_1$$
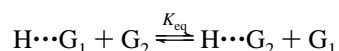
as $K_{eq} = [G_1]K_{assoc}(G_1)/[G_2]K_{assoc}(G_2)$. For the pre-PET exchange of HTEOA⁺ (G₁) by MV²⁺ (G₂) with [Ru^II(**1**)(bpy)₂]⁺ (H), where [HTEOA⁺] is at most equal to [Ru] because it forms by deprotonation of the host, K_{eq} reaches up to 217. But the associations are weak, and at the concentrations used and assuming 100% ionization of the COOH groups, one can compute that at most 5.6% of the sensitizer is paired up with MV²⁺. It is therefore likely that PET with singly carboxylated sensitizers occurs by a mix of a more efficient unimolecular path and a less efficient but more probable bimolecular path. The post-PET exchanges at this same host of MV•⁺ (G₁) by HTEOA⁺ or MV²⁺ (G₂), where [MV•⁺] is at most 1% of

[MV²⁺] according to Table 1, are also favorable, with $K_{eq} \approx$ 1.1 or 68, respectively. The associations are weaker still, and the exchange is driven by concentration differences. The majority of the Ru photoproduct will therefore be mostly unassociated or inconsequently associated with MV²⁺ and HTEOA⁺, rather than with MV•⁺, and the reverse electron transfer (BET) will then be largely bimolecular. Not included in this analysis is the possible participation of the cationic sensitizer molecules themselves in the cation exchanges nor the effect of PF₆⁻. Usually accorded a role as spectator counterion, PF₆⁻ can engage in a weak association with HTEOA⁺, providing additional motivation for the deprotonation of COOH groups by TEOA and for the displacement of HTEOA⁺ by MV²⁺.

Figure 5 and Table 3 present the electrostatic fields and dissociation energies for dicarboxylated complexes. With Ru^II, the sensitizers are neutral and the carboxylate groups define entire sectors of attractive space, instead of confined bubbles, but these collapse to bubbles after PET when the complexes become cationic. The shapes of the attractive sectors/bubbles, depicted in Figure 5, depend on *r*, the COO⁻⋯COO⁻ separation. At one extreme, with **7**⁻, there are two independent cones of attractive space with Ru^II that shrink to independent bubbles with Ru^III. At the other extreme, with **1**⁻ or **8**⁻, the entire sector adjoining the carboxylates is attractive with Ru^II and this shrinks with Ru^III to a kidney shape in which the individual bubbles have melded. In the intermediate case, with **3**²⁻, this melding is incomplete. The optimal orientations of MV²⁺/MV•⁺ before PET are also depicted in Figure 5. Clearly, two-point binding occurs with **1**⁻ (and **8**⁻, not depicted) but not in the other two cases, where the carboxylates are too far apart and more independent. These findings are reflected in the calculated *E* values listed in Table 3.

An important question is what benefit is there in providing additional COO⁻ binding sites, especially in regard to the selectivity for pre- versus post-PET binding. This can be assessed by considering the *E* values from Tables 2 and 3 for the binding of single guests. The *E* values all increase with additional carboxylation, the size of the increase being larger with decreasing *r*. With one ligand **1**⁻, the Ru^II state binds HTEOA⁺ more strongly than does the Ru^III state, by 3.76 kJ

Table 3. Dissociation Energies E (kJ mol^{-1}) of Guests from Dicarboxylated Complexes of M$^{II/III}$ and L, against Their COO$^-$···COO$^-$ Separations r (Å)

L	1$^-$		8$^-$		3^{2-}		7$^-$	
r (Å)	9.22		9.36		12.76		21.1	
oxidn state	II	III	II	III	II	III	II	III
MV^{2+} ^{a}	20.22	11.21	18.28	8.17	9.63	2.60	11.47	6.17
2MV^{2+}					15.36	1.31	18.92	7.62
HTEOA$^+$	9.29	5.22	8.37	4.26	7.62	3.83	8.80	6.05
2HTEOA$^+$	15.29	7.80	14.38	6.40	14.12	6.54	16.91	11.41
MV^{2+} + HTEOA$^+$	20.02	6.49	17.82	3.04	15.11	4.30	18.88	10.83
MV$^{\bullet+}$ + MV^{2+}						2.03		7.95
MV$^{\bullet+}$ + HTEOA$^+$		4.79		2.77		4.06		8.44

^{a} Values for MV$^{\bullet+}$ will be half those for MV^{2+}.

mol^{-1} (Table 2). With two **1**$^-$, that difference increases to 4.07 kJ mol^{-1} (Table 3), for a net benefit to the selectivity of 0.31 kJ mol^{-1} upon addition of the second COO$^-$ group. The benefit of additional carboxylation with ligand **8**$^-$ is weaker (0.11 kJ mol^{-1}) because r is longer, albeit by only a fraction of an angstrom, and s is shorter. With ligands **7**$^-$ and H**3**$^-$/**3**$^{2-}$, r is too long and the net benefit from additional carboxylation is vanishingly small. The net benefits pertaining to the selectivities for Ru^{II}/MV^{2+} over Ru^{III}/MV$^{\bullet+}$ combinations are much larger but, again, decrease rapidly with increasing r.

One interesting result from the computations of E revealed in Table 3 is the finding that [Ru$^{II/III}$(**3**)(H$_2$**3**)]^0 is the weakest host. An analysis of the components of F showed that the other complexes bind guests more strongly because their Ru···N$^+$ repulsions are weaker, as with ligand **7**$^-$, or because their distal COO$^-$···N$^+$ attractions are stronger, as with **1**$^-$ and **8**$^-$, and the guests tilt accordingly. In general, the binding of a second guest is weakened by N$^+$–N$^+$ repulsion and the tilt angles are reduced. However, the E values for two guests are still greater than twice the values for one such guest bound to the monocarboxylated analogues (Table 2) because the attraction of any one guest to the second, distal COO$^-$ group compensates for the new N$^+$···N$^+$ repulsion between guests, which in any case is minimized by tilting ($\theta \neq 0$).

As was true with singly carboxylated sensitizers, Table 3 indicates that the dissociation of MV$^{\bullet+}$ after PET is always easier than that of MV^{2+} before PET with doubly carboxylated hosts. As well, the exchanges of two HTEOA$^+$ by MV^{2+} before PET and of MV$^{\bullet+}$ by MV^{2+} or by two HTEOA$^+$ after PET are all favorable where two-point binding can occur. Indeed, with **1**$^-$ or **8**$^-$, the exchange of MV$^{\bullet+}$ by a single HTEOA$^+$ is unfavorable, as the two-point binding of MV$^{\bullet+}$ is incompletely replaced by the one-point binding of HTEOA$^+$. Complexes [Ru-(H$_2$**3**)(**3**)]^0 and [Ru(**7**)$_2$]^0, on the other hand, behave much as if they were monocarboxylated. These findings also hold for charge-localized MV$^{\bullet+}$ in all cases.

Scheme 3 illustrates the exchange pathways and their relative energetic costs in a favorable case, with [Ru(**1**)$_2$(bpy)]^0. After PET, the exchanges of MV$^{\bullet+}$ to restore MV^{2+} are favorable. Analogous schemes were constructed for the other complexes of Table 3 (Supporting Information). That with ligand **8**$^-$ is entirely similar to Scheme 3, but the other two cases, where there is only one-point binding, differ in that two guests can be present, photochemistry can occur with one or two MV^{2+} guests present, and the driving forces for the exchanges are all much weaker. The post-PET exchanges of MV$^{\bullet+}$ by MV^{2+} in these cases are favorable only if the other guest is monocationic (HTEOA$^+$). As with the monocarboxylated cases, the ordering

Scheme 3. Species Involved in Productive Reactions 1 and 2 (from Scheme 1) via Cation Exchange Steps (Marked CE), with [Ru(H**1**)$_2$(bpy)]$^{2+a}$
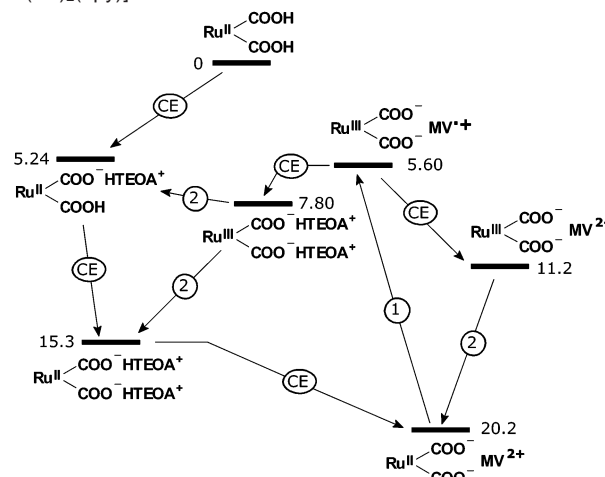
^{a} Ranked according to E (kJ mol^{-1}). The value for the singly deprotonated HTEOA$^+$ salt is from Table 2.

depicted in Scheme 3 was found to be robust toward errors in d (Supporting Information).

As before with Scheme 2, we can calculate for Scheme 3 that COOH ionization affords a stabilization of about 33 kJ mol^{-1} pre-PET versus about 15 kJ mol^{-1} post-PET. As well, we can estimate K_{assoc} at about 2900 M^{-1} with MV^{2+} pre-PET versus 8 M^{-1} with MV$^{\bullet+}$ post-PET (cf. 76.3 M^{-1} with MV^{2+} post-PET), with the consequence that the vast majority (>96%) of [Ru^{II}(H**1**)$_2$(bpy)]$^{2+}$ will be associated with MV^{2+} if it is 100% ionized, so that PET with this species is probably mostly unimolecular. After PET, favorable binding and concentration factors mean that the Ru photoproduct will much prefer to bind MV^{2+}, rather than MV$^{\bullet+}$ or HTEOA$^+$. For instance, $K_{eq} \approx 950$ for the post-PET exchange of MV$^{\bullet+}$ by the abundant MV^{2+}, which will end up taking care of some 42% of the host [Ru^{III}-(**1**)$_2$(bpy)]$^+$, leaving most of it without a guest. BET will therefore remain largely bimolecular, just as with the monocarboxylated hosts.

The associative work terms W of eq 2 correspond to $-E$ in our dissociation energy formalism but refer to Ru^{II} excited states and Ru^{III} ground states. Using $-E$ is appropriate for the latter, but as a simplifying assumption for the former, we can use the $-E$ values from the Ru^{II} ground states for comparisons between sensitizers.[41] Table 4 reports the calculated values of ΔG^* for both PET and BET with some mono- and dicarboxylated

(40) Kavarnos, G. J. *Fundamentals of Photoinduced Electron Transfer*; VCH: New York, 1993; p 310.

Table 4. Estimations of the Energies of Activation for Electron Transfer, ΔG^*

	Λ^a /eV	W_R /eV	W_P /eV	$E_{ox}{}^b$ /V	λ_{max} /nm	$\Delta G°_{PET}{}^c$ /eV	$\Delta G°_{BET}$ /eV	ΔG^*_{PET} /eV	ΔG^*_{BET} /eV
$[Ru(bpy)_3]^{2+}$	0.955	0.149	0.112	1.26	454	−0.42	−1.71	0.21	0.25
$[Ru(ttpy)_2]^{2+}$	0.955	0.149	0.112	1.25^d	490^d	−0.24	−1.70	0.27	0.24
$[Ru(\mathbf{1})(bpy)_2]^+$	0.953	−0.052	0.010	1.25^e	449^e	−0.45	−1.70	0.031	0.18
$[Ru(\mathbf{7})(ttpy)]^+$	0.970	−0.087	0.016	1.25^f	490^f	−0.24	−1.70	0.093	0.19
$[Ru(\mathbf{H8})(\mathbf{8})]^{+\,g}$	0.952	−0.044	0.016	1.39^d	492^d	−0.07	−1.84	0.19	0.25
						[−0.21]	[−1.70]	[0.13]	[0.19]
$[Ru(\mathbf{1})_2(bpy)]^0$	0.953	−0.210	−0.058	1.20^e	450^e	−0.49	−1.65	−0.11	0.13
$[Ru(\mathbf{7})_2]^0$	0.970	−0.119	−0.032	1.25^f	490^f	−0.24	−1.70	0.054	0.14
$[Ru(\mathbf{8})_2]^{0\,g}$	0.952	−0.189	−0.042	1.39^d	492^d	−0.07	−1.84	0.089	0.24
						[−0.21]	[−1.70]	[0.019]	[0.17]
$[Ru(dcbpy)(bpy)_2]^0$	0.952	−0.211	−0.060	1.27^h	457^h	−0.33	−1.72	−0.055	0.16

^{a} $\Lambda \approx \Lambda_{out} = e^2(^1/_2R_A + {}^1/_2R_B - 1/(R_A + R_B))(1/n^2 - 1/\rho)$ (ref 35). The refractive index n for CH_3CN is 1.3441, and its dielectric constant ρ is 37.5. Using the s values of Table 2, $R_A = s + 2.9/2$ Å (see text) or 7 Å for $[Ru(bpy)_3]^{2+}$ or $[Ru(ttpy)_2]^{2+}$, and $R_B = 3.3$ Å (ref 38). ^{b} $E(Ru^{III/II})$ values vs SCE. When not available, the corresponding values from ester forms were used. ^{c} Equation 3 used. E_{00} for $[Ru(bpy)_3]^{2+}$ is 2.12 eV (Balzani, V.; Barigelletti, F.; De Cola, L. *Top. Curr. Chem.* **1990**, *158*, 31). E_{00} for $[Ru(ttpy)_2]^{2+}$ and $[Ru(dcbpy)(bpy)_2]^0$ were calculated at 1.94 and 2.05 eV from their emission λ_{max} at 640 nm (Barigelletti, F.; Flamigni, L.; Balzani, V.; Collin, J.-P.; Sauvage, J.-P.; Sour, A.; Constable, E. C.; Cargill Thompson, A. M. W. *J. Chem. Soc., Chem. Commun.* **1993**, 942) and 604 nm (ref 42), respectively. E_{00} for the other cases are taken to be the same as that for $[Ru(bpy)_3]^{2+}$ or $[Ru(ttpy)_2]^{2+}$, with correction for any drop in MLCT energy. ^{d} Data from ref 3. ^{e} Data from ref 20. ^{f} Taken to be the same as for $[Ru(ttpy)_2]^{2+}$. ^{g} E_{ox} value of the diester used. Values in square brackets are obtained with the E_{ox} value of $[Ru(ttpy)_2]^{2+}$. ^{h} Data from ref 42.

sensitizers in comparisons with $[Ru(bpy)_3]^{2+}$ and $[Ru(ttpy)_2]^{2+}$. Data for $[Ru(dcbpy)(bpy)_2]^0$ are also included for comparison, using E values computed in exactly the same manner as for the other complexes. To make comparisons between all complexes and to explore electrostatic effects, only bimolecular electron transfers were considered. This shows that both PET and BET are strongly facilitated as a result of carboxylation, relative to the non-carboxylated analogues. Moreover, the forward reaction is favored ($\Delta G^*_{PET} < \Delta G^*_{BET}$) for all carboxylated cases. The ΔG^* values with ligand $\mathbf{8}^-$ are exceptional, and this can be traced to the high E_{ox} value used in the calculations. As no experimental E_{ox} value was available, the value from the diester precursor[3] was used, and this is shifted positive because the electron-withdrawing ester groups are on the metal-bound pyridine rings. The ΔG^* values resulting are probably overestimates, as E_{ox} probably drops closer to the value from $[Ru(ttpy)_2]^{2+}$ in the deprotonated species as COO^- groups are more weakly electron withdrawing. The bracketed values in Table 4 are recalculations using the E_{ox} value of $[Ru(ttpy)_2]^{2+}$ for the complexes of $\mathbf{8}^-$, bringing their results more in line with the others. Interestingly, ΔG^*_{PET} is < 0 for the strongest-binding hosts, $[Ru(\mathbf{1})_2(bpy)]^0$ and $[Ru(dcbpy)(bpy)_2]^0$, where the first term of eq 2 is larger than the second, as if the electrostatic stabilization gained upon bimolecular collision to form the transition state is sufficient to overcome the barrier to electron transfer. Importantly, the difference in activation energies between forward and reverse electron transfers, $\Delta G^*_{BET} - \Delta G^*_{PET}$, which can be related to the efficiency of photoproduct accumulation, increases substantially as a result of carboxylation.

The ΔG^* values of Table 4 are approximations, for which a certain number of assumptions were needed, and though they are calculable factors, they are not the sole factors accounting for the observed rates. The ΔG^*_{PET} values correlate well with both ln k_{init} ($r^2 > 0.96$) and ln k_f ($r^2 > 0.94$) for the five *nonluminescent* complexes of Table 4 (the singly deprotonated $[Ru(\mathbf{H8})(\mathbf{8})]^+$ is not included in this collection, since it is hypothetical and we have no kinetic data for it). As discussed

earlier, the E_{ox} value for $[Ru(\mathbf{8})_2]^0$ was taken as 1.25 V. The luminescent cases, $[Ru(bpy)_3]^{2+}$ and $[Ru(\mathbf{1})(bpy)_2]^+$, which owe most of their success to higher τ values, do not fit these correlations. With these limitations, the calculations nevertheless seem to reflect well the electrostatic benefits of carboxylation.

4. Discussion

The principal findings of this study are four-fold. First, all complexes explored were able to photogenerate $MV^{\bullet+}$ in measurable amounts, even if most are not luminescent at room temperature. On the basis that all are similar in constitution and structure, with similar MLCT λ_{max}, ϵ, emission λ_{max}, and similar $E_{1/2}(Ru^{III/II})$ values, the differences in luminescence intensity that they show may be attributed mostly to differences in excited-state lifetimes τ. The strongly luminescent $Ru(bpy)_3{}^{2+}$ and the nonluminescent $Ru(ttpy)_3{}^{2+}$ ($\tau = 0.95$ ns in nitrile solvent)[43] then provide a scale against which the other complexes can be gauged. Because the method used here directly measures photoproduct formation, it is a useful, direct, and easier assessment of sensitizer ability than measurements of τ or of luminescence quenching rates and appears to be applicable to materials of widely varying τ.

Second, the initial rate constants k_{init} were found to be reliable predictors of k_f. Because k_{init} is easier to evaluate than k_f, k_{init} values might be employed alone in rapid screenings of large numbers of samples. This finding also validates the previous practice of measuring the initial rates of $MV^{\bullet+}$ generation in H_2O.[44]

Third, only the good sensitizers showed any activity in aqueous media, and so the solvent is an important effector of activity. For example, the very weakly luminescent $[Ru(Na\mathbf{1})_2(bpy)]^{2+}$ (emission λ_{max} 598 nm)[24] showed complete inactivity in H_2O and negligible activity in 80% CH_3CN, all consonant with a very short τ, but showed appreciable activity in pure CH_3CN (Figure 2).

(41) Modeling the electrostatics with Ru^{II} excited states is difficult. They are MLCT states with Ru^{III} and a reduced ligand. The E values will be underestimates if the reduced ligand is closer to the guest than the metal, as with $[Ru(\mathbf{1})_2(bpy)]^+$, and overestimates otherwise.

(42) Xie, P.-H.; Hou, Y.-J.; Zhang, B.-W.; Cao, Y.; Wu, F.; Tian, W.-J.; Shen, J.-C. *J. Chem. Soc., Dalton Trans.* **1999**, 4217.

(43) Barigelletti, F.; Flamigni, L.; Balzani, V.; Collin, J.-P.; Sauvage, J.-P.; Sour, A.; Constable, E. C.; Cargill Thompson, A. M. W. *J. Chem. Soc., Chem. Commun.* **1993**, 942.

(44) Mandal, K.; Hoffman, M. Z. *J. Phys. Chem.* **1984**, *88*, 185. Georgopoulos, M.; Hoffman, M. Z. *J. Phys. Chem.* **1991**, *95*, 7717. Sun, H.; Hoffman, M. Z. *J. Phys. Chem.* **1994**, *98*, 11719.

Fourth, the carboxylated complexes all showed higher activities in CH_3CN than their non-carboxylated analogues. This can be explained by a preassociation of the photoreactants and by cation exchanges that facilitate this preassociation and the dissociation of the photoproducts. Even single carboxylation suffices to dramatically improve the electrostatic situation by these means. The interactions involved are substantiated by computations of the electrostatic forces at play, the resultant dissociation energies, and electron-transfer activation energies.

4.1. Excited-State Lifetime. The prior literature offers examples of charge effects on PET in aqueous media: aqueous solutions of carboxylated[15] and sulfonated[16] bipyridine complexes showed faster rates of PET to cationic acceptors, and negative salt effects indicated a useful association between the photoreactants.[15] The ground-state coordination of carboxylated, sulfonated, or phosphonated sensitizers to Cu^{2+} or Fe^{3+} served to explain the efficient quenching by these ions of the sensitizer luminescence.[16,45] Recent work has shown that PET to semiconductor particles can proceed from even extremely short-lived excited states with the help of attractive interactions between the sensitizer and the semiconductor surface,[46] and ionizable groups are now routinely used for anchoring sensitizers to such surfaces.[47] Such interactions are evidently or arguably short-range phenomena, as in the case of the ion−dipole interactions between MV^{2+} and a $[Ru(bpy)_3]^{2+}$ modified with polyether side chains.[48] Indeed, long-range electrostatic interactions are weakened in H_2O by charge dispersal in the highly dielectric medium and by tight binding of counterions (PF_6^-, $HTEOA^+$) in CH_3-CN.

Ligand carboxylation and ionization are known to also influence τ. However, the literature does not indicate more than a small effect. Generalizations are difficult to make because different solvents have often been used in different cases. There is disagreement on the effect of 4/4′-carboxylation on $[Ru(bpy)_3]^{2+}$, with τ measurements showing a decrease,[15] no change,[16] or an increase.[49] At best, six COO^- groups at the 4/4′ positions of $[Ru(bpy)_3]^{2+}$ resulted in a 29% longer τ, the same level of improvement seen with 4-carboxyphenyl substituents.[49] This is a much smaller increase than those revealed in Table 1 by comparison of the k_f or k_{init} values of the carboxylated sensitizers and their non-carboxylated analogues. Carboxylation was found to be severely detrimental[42,49] at the 5/5′ positions but less so at 3/3′,[42] while carboxylation at C-6 was mildly so.[32] Nevertheless, a general finding from these and other[50] reports is that electron-withdrawing groups tend to lengthen τ, and COO^- groups act as weak electron withdrawers. There exist counterexamples, however.[51] In our case, steric considerations and crystal structures[20,52] indicate that the carboxyphenyl side chains of **1** or **3** must lie perpendicular to the ligand plane, with poor π overlap, so that the side chains constitute modest σ withdrawers, with modest effects expected on the complex τ. Table 4 includes $[Ru(4)_2]^{2+}$, which bears σ-withdrawing ester substituents, and analogue $[Ru(5)_2]^{2+}$, with σ-donating CH_3 groups. The difference in activity between these is slight, actually favoring the latter complex, and much smaller than between carboxylated and non-carboxylated sensitizers. Hence, the electronic influence on τ from side-chain substituents here therefore seems too small to account for the increased activity afforded by COO^- groups.

There is a generally beneficial effect on τ values and quenching rates upon using an organic solvent. Few sensitizers have been studied in more than one solvent, and the results are sometimes at variance or difficult to rationalize. In particular, the measurements of τ for $[Ru(bpy)_3]^{2+}$ in various solvents are scattered as are the rate constants for the quenching of its excited state by MV^{2+}. The τ value is 1.2−2.2 times larger in CH_3-CN[13] than in H_2O,[10] depending on the measurements compared, while the second-order rate constants for quenching by MV^{2+} in H_2O[53] and CH_3CN[56] are very scattered, indicating a solvent-induced change of as little as 1.6-fold or as much as 7.1-fold.

(45) Montalti, M.; Wadhwa, S.; Kim, W. Y.; Kipp, R. A.; Schmehl, R. H. *Inorg. Chem.* **2000**, *39*, 76.
(46) Vlachopoulos, N.; Liska, P.; Augustynski, J.; Grätzel, M. *J. Am. Chem. Soc.* **1988**, *110*, 1216. Kohle, O.; Ruile, S.; Grätzel, M. *Inorg. Chem.* **1996**, *35*, 4779. Argazzi, R.; Bignozzi, C. A.; Hasselman, G. M.; Meyer, G. J. *Inorg. Chem.* **1998**, *37*, 4533. Kalyanasundaram, K.; Grätzel, M. *Coord. Chem. Rev.* **1998**, *77*, 347.
(47) Meyer, T. J.; Meyer, G. J.; Pfennig, B. W.; Schoonover, J. R.; Timpson, C. J.; Wall, J. F.; Kobusch, C.; Chen, X.; Peek, B. M. *Inorg. Chem.* **1994**, *33*, 3952. Argazzi, R.; Bignozzi, C. A.; Heimer, T. A.; Castellano, F. N.; Meyer, G. J. *Inorg. Chem.* **1994**, *33*, 5741. Argazzi, R.; Bignozzi, C. A.; Heimer, T. A.; Castellano, F. N.; Meyer, G. J. *J. Am. Chem. Soc.* **1995**, *117*, 11815. Vinodgopal, K.; Hua, X.; Dahlgren, R. L.; Lappin, A. G.; Patterson, L. K.; Kamat, P. V. *J. Phys. Chem.* **1995**, *99*, 10883. Fessenden, R. W.; Kamat, P. V. *J. Phys. Chem.* **1995**, *99*, 12902. Pechy, P.; Rotzinger, F. P.; Nazeeruddin, M. K.; Kohle, O.; Zakeeruddin, S. M.; Humphry-Baker, R.; Grätzel, M. *J. Chem. Soc., Chem. Commun.* **1995**, 65. Heimer, T. A.; D'Arcangelis, S. T.; Farzad, F.; Stipkala, J. M.; Meyer, G. J. *Inorg. Chem.* **1996**, *35*, 5319. Zakeeruddin, S. M.; Nazeeruddin, M. K.; Pechy, P.; Rotzinger, F. P.; Humphry-Baker, R.; Kalyanasundaram, K.; Grätzel, M.; Shklover, V.; Haibach, T. *Inorg. Chem.* **1997**, *36*, 5937. Striplin, D. R.; Wall, C. G.; Erickson, B. W.; Meyer, T. J. *J. Phys. Chem. B* **1998**, *102*, 2383. Falaras, P.; Xagas, A. P.; Hugot-Le Goff, A. *New J. Chem.* **1998**, *22*, 557. Trammell, S. A.; Meyer, T. J. *J. Phys. Chem. B* **1999**, *103*, 104. Nazeeruddin, M. K.; Zakeeruddin, S. M.; Humphry-Baker, R.; Jirousek, M.; Liska, P.; Vlachopoulos, N.; Shklover, V.; Fischer, C.-H.; Grätzel, M. *Inorg. Chem.* **1999**, *38*, 6298. Takahashi, Y.; Arakawa, H.; Sugihara, H.; Hara, K.; Islam, A.; Katoh, R.; Tachibana, Y.; Yanagida, M. *Inorg. Chim. Acta* **2000**, *310*, 169. Xie, P.-H.; Hou, Y.-J.; Wei, T.-X.; Zhang, B.-W.; Cao, Y.; Huang, C.-H. *Inorg. Chim. Acta* **2000**, *308*, 73. Sayama, K.; Hara, K.; Mori, N.; Satsuki, M.; Suga, S.; Tsukagoshi, S.; Abe, Y.; Sugihara, H.; Arakawa, H. *J. Chem. Soc., Chem. Commun.* **2000**, 1173. Islam, A.; Sugihara, H.; Hara, K.; Singh, L. P.; Katoh, R.; Yanagida, M.; Takahashi, Y.; Murata, S.; Arakawa, H. *New J. Chem.* **2000**, *24*, 343. Yanagida, M.; Singh, L. P.; Sayama, K.; Hara, K.; Katoh, R.; Islam, A.; Sugihara, H.; Arakawa, H.; Nazeeruddin, M. K.; Grätzel, M. *J. Chem. Soc., Dalton Trans.* **2000**, 2817.
(48) Bossmann, S.; Seiler, M.; Dürr, H. *J. Phys. Org. Chem.* **1992**, *5*, 63. Seiler, M.; Dürr, H.; Willner, I.; Joselevich, E.; Doron, A.; Stoddart, J. F. *J. Am. Chem. Soc.* **1994**, *116*, 3399. Kropf, M.; Joselevich, E.; Dürr, H.; Willner, I. *J. Am. Chem. Soc.* **1996**, *118*, 655. Kropf, M.; Dürr, H.; Collet, C. *Synthesis* **1996**, 609.
(49) Kalyanasundaram, K.; Nazeeruddin, M. K.; Grätzel, M.; Viscardi, G.; Savarino, P.; Barni, E. *Inorg. Chim. Acta* **1992**, *198*, 831.
(50) Wacholz, W. F.; Auerbach, R. A.; Schmehl, R. H. *Inorg. Chem.* **1986**, *25*, 227. Constable, E. C.; Cargill-Thompson, A. M. W.; Tocher, D. A.; Daniels, M. A. *New J. Chem.* **1992**, *16*, 855. Constable, E. C.; Cargill-Thompson, A. M. W.; Amaroli, N.; Balzani, V.; Maestri, M. *Polyhedron* **1992**, *20*, 2707. Amouyal, E.; Mouallem-Bahout, M.; Calzaferri, G. *J. Phys. Chem.* **1991**, *95*, 7641. Maestri, M.; Amaroli, N.; Balzani, V.; Constable, E. C.; Cargill-Thompson, A. M. W. *Inorg. Chem.* **1995**, *34*, 2759. Zakeeruddin, S. M.; Nazeeruddin, M. K.; Pechy, P.; Rotzinger, F. P.; Humphry-Baker, R.; Kalyanasundaram, K.; Grätzel, M.; Shklover, V.; Haibach, T. *Inorg. Chem.* **1997**, *36*, 5937.
(51) Cook, M. J.; Lewis, A. P.; McAuliffe, G. S. G.; Skarda, V.; Thomson, A. J.; Glasper, J. L.; Robbins, D. J. *J. Chem. Soc., Perkin Trans. 2* **1984**, 1293.
(52) Luo, Y.; Potvin, P. G. *J. Coord. Chem.* **1999**, *46*, 319.
(53) Values reported for the second-order rate constant in H_2O (M^{-1} s^{-1}) include 2.8×10^8 (ref 16), 4.5×10^8 (ref 54), 5.0×10^8 (ref 55), 6.2×10^8 (ref 12), 1.0×10^9 (ref 11), and 1.7×10^9 (Nishijima, T.; Nagamura, T.; Matsuo, T. *J. Polym. Sci, Polym. Lett. Ed.* **1981**, *19*, 65); higher values have been reported in the presence of added electrolytes (refs 9, 15; Kitamura, N.; Kawanishi, Y.; Tazuke, S. *Chem. Lett.* **1983**, 1185; Ochiai, E.-I.; Shaffer, D. I.; Wampler, D. L.; Schettler, P. D., Jr. *Transition Met. Chem.* (Weinheim, Germany) **1986**, *11*, 241).
(54) Sassoon, R. E.; Gershuni, S.; Rabani, J. *J. Phys. Chem.* **1985**, *89*, 1937.
(55) Kalyanasundaram, K.; Neumann-Spallart, M. *Chem. Phys. Lett.* **1982**, *88*, 7.
(56) Values reported for the second-order rate constant in CH_3CN (M^{-1} s^{-1}) include 2.0×10^9 (ref 55), 2.4×10^9 (ref 57; Bock, C. R.; Connor, J. A.; Gutierrez, A. R.; Meyer, T. J.; Whitten, D. G.; Sullivan, B. P.; Nagle, J. K. *J. Am. Chem. Soc.* **1979**, *101*, 4815; Bolletta, F.; Maestri, M.; Balzani, V. *J. Phys. Chem.* **1976**, *80*, 2499) and 2.8×10^9 (ref 14).

The τ value in EtOH[58] is comparable to that in CH$_3$CN,[13] but the rate constant for quenching by MV^{2+} is nearly an order of magnitude lower in EtOH[58] than in CH$_3$CN.[56] With [Ru(bpy)$_2$-(decbpy)]$^{2+}$ (decbpy is 4,4′-diethoxycarbonyl-2,2′-bipyridine)[58] and with the neutral Ru(bpy)$_2$(CN)$_2$,[59,60] both τ and the quenching rates also increased in CH$_3$CN relative to H$_2$O, but by factors < 3. Increases in quenching rates are necessarily restricted by the diffusion limit, as in the latter case. In comparison, k_{init} for [Ru(**1**)(bpy)$_2$]$^+$ in H$_2$O increased by a factor of 7.5 in CH$_3$CN. With [Ru(bpy)$_3$]$^{2+}$, k_{init} increased by a factor of 2.4. The case of [Ru(Na**1**)$_2$(bpy)]$^{2+}$ was even more dramatic, since it was totally inactive in H$_2$O even though the dissociation of Na$^+$ produces an overall neutral species. In general, it may be concluded that the sensitizers which showed no activity in H$_2$O despite favorable electrostatics must have exceedingly short τ values. While the solvent-induced increase can be entirely ascribed to a solvent effect with [Ru(bpy)$_3$]$^{2+}$, this is not reasonably done for [Ru(**1**)(bpy)$_2$]$^+$ and [Ru(Na**1**)$_2$(bpy)]$^{2+}$, where electrostatic effects must play a role.

4.2. Supramolecular Assistance with Monocarboxylation. Superficially, both PET and BET with a monocationic sensitizer involve monocation—dication encounters, and no electrostatic advantage nor disadvantage would be accorded either, relative to the other. On the contrary, we find that the electrostatic field surrounding a carboxylated complex provides PET with an advantage over BET for two reasons. First, the interaction of a monocarboxylated complex such as [Ru^{II}(**1**)(bpy)$_2$]$^+$ with MV^{2+} is mildly attractive at close range, despite the overall charge, because the COO$^-$ group is on the accessible periphery and forms an electrostatically attractive "bubble" large enough to constitute a binding site for MV^{2+} (Figure 4). As computed in section 2.4, the minimum Ru^{2+}···COO$^-$ separation for this to be so will always be met. As testament to the existence and effect of such "bubbles", we note that the product of the NaOH digestion (and subsequent anion exchange) of the diester [Ru^{II}-(**6**)$_2$(bpy)](PF$_6$)$_2$ was not the internally charge-compensated species [Ru^{II}(**1**)$_2$(bpy)]^0 but the double NaPF$_6$ adduct, [Ru^{II}-(Na**1**)$_2$(bpy)](PF$_6$)$_2$. Carboxylated sensitizers and MV^{2+} can therefore associate within the bubbles *prior to* the photoevent to an appreciable degree, leading to static quenching, at least in part (we estimated in section 3.3 that 5.6% of the [Ru(**1**)-(bpy)$_2$]$^+$ can undergo static quenching in CH$_3$CN). This would provide an entropic advantage over the bimolecular process, in which the reactants must instead collide after the photoexcitation step (dynamic quenching),[61] the probability for which depends on τ. A preassociation would thus reduce the need for a long-lived excited state. (Aqueous solvents would reduce this benefit, all the more at high salt concentrations.)[15,62] According to Table 2 and Scheme 2, this preassociation can occur by facile cation exchanges.

The second reason that PET is electrostatically favored over BET is that the cation-attractive space available before PET shrinks dramatically as a result of PET (Figure 4); the interaction between photoproducts becomes repulsive much nearer the complex and is furthermore stronger outside the smaller bubble. As substantiated by dissociation energy and association constant estimates, this would facilitate photoproduct separation upon diffusional collision, reducing the danger of BET (Scheme 1, reaction 5) before the Ru^{3+} can be removed and recycled (Scheme 1, reaction 2). According to Scheme 2 and Table 2, cation exchange provides a mechanism for the diffusion of MV$^{•+}$. An exchange by HTEOA$^+$ provides the additional opportunity to simultaneously reduce the Ru^{III} to Ru^{II}, further helping to accumulate MV$^{•+}$.

Thus, we conclude that carboxylation converts a system in which BET is electrostatically favored over PET to one where the opposite is true, one where some preassociation can occur through counterion exchange and result in some unimolecular quenching. The benefits of this are exemplified by [Ru(**7**)-(ttpy)]$^+$, with about twice the photoproduct yield of its non-carboxylated analogue [Ru(ttpy)$_2$]$^{2+}$. The other singly carboxylated example is [Ru(**1**)(bpy)$_2$]$^+$. While we have no strictly analogous non-carboxylated version for comparison, we can nevertheless compare the relative activities of [Ru(**1**)(bpy)$_2$]$^+$ and [Ru(bpy)$_3$]$^{2+}$: despite an evidently less favorable τ, [Ru-(**1**)(bpy)$_2$]$^+$ is the better sensitizer in CH$_3$CN, while the reverse is true in aqueous solvents. Above and beyond any solvent effect on τ, which should affect both sensitizers, this is because of the electrostatic benefits available to [Ru(**1**)(bpy)$_2$]$^+$ and not available to [Ru(bpy)$_3$]$^{2+}$, benefits which are accessible in CH$_3$-CN but greatly diluted in aqueous media.

Because two cations are not expected to associate at all, the attractive interactions at issue here between cationic photoreactants can be considered *supramolecular* in nature, involving weak, noncovalent bonds at close range in much the same way as do the hydrogen bonds at the basis of more common supramolecular assemblies. We had previously obtained indirect evidence of such supramolecular interactions: Already mentioned is the double NaPF$_6$ adduct, [Ru(Na**1**)$_2$(bpy)](PF$_6$)$_2$, a union of three formally neutral species. Second, we had found that a 1:1 mixture of [Ru(Na**1**)$_2$(bpy)](PF$_6$)$_2$ and MV(PF$_6$)$_2$ in CD$_3$CN showed severely broadened ^{1}H NMR signals and small upfield shifts of several signals, notably that from C−H adjoining the COO$^-$ groups.[24] Third, at concentrations much higher than those used here, [Ru(H$_2$**3**)$_2$]$^{2+}$ and MV^{2+} in the presence of base coprecipitated as a supramolecular aggregate of formula MV[Ru(**3**)(H**3**)]$_2$.[21]

This supramolecular effect is distinct from the effect of anionic ligands, such as halides or pseudohalides,[15,26,63] β-diketonates,[64] cyanamides,[65] phthalocyanines,[18,66] porphyrins,[67] and other N−H acidic ligands[20,21] that "covalently" weaken, elimi-

(57) Young, R. C.; Meyer, T. J.; Whitten, D. G. *J. Am. Chem. Soc.* **1976**, *98*, 286.

(58) Johansen, O.; Launikonis, A.; Mau, A. W.-H.; Sasse, W. H. F. *Aust. J. Chem.* **1980**, *33*, 1643.

(59) Values reported for *cis*-Ru(bpy)$_2$(CN)$_2$ include 0.26 μs in H$_2$O (ref 15) and 0.34 μs in CH$_3$CN (ref 57).

(60) Values reported (M^{-1} s^{-1}) for *cis*-Ru(bpy)$_2$(CN)$_2$ include 9.2 × 10^9 in CH$_3$-CN (ref 57), 4.1 × 10^9 in H$_2$O (ref 54), and 5.3 × 10^9 in H$_2$O (ref 15).

(61) Sutin, N. *J. Photochem.* **1979**, *10*, 19. Kavarnos, G. J. *Top. Curr. Chem.* **1990**, *156*, 21. Balzani, V.; Scandola, F. In *Energy Resources Through Photochemistry and Catalysis*; Grätzel, M., Ed.; Academic Press: New York, 1983; p 1.

(62) Bolletta, F.; Maestri, M.; Moggi, L.; Balzani, V. *J. Am. Chem. Soc.* **1973**, *95*, 7864.

(63) Jing, B.; Zhang, H.; Zhang, M.; Lu, Z.; Shen, T. *J. Mater. Chem.* **1998**, *8*, 2055. Yanagida, M.; Singh, L. P.; Sayama, K.; Hara, K.; Katoh, R.; Islam, A.; Sugihara, H.; Arakawa, H.; Nazeeruddin, M. K.; Grätzel, M. *J. Chem. Soc., Dalton Trans.* **2000**, 2817.

(64) Takahashi, Y.; Arakawa, H.; Sugihara, H.; Hara, K.; Islam, A.; Katoh, R.; Tachibana, Y.; Yanagida, M. *Inorg. Chim. Acta* **2000**, *310*, 169.

(65) Crutchley, R. J.; Naklicki, M. L.; White, C. A.; Kondratiev, V. V. *Inorg. Chim. Acta* **1996**, *242*, 63. Crutchley, R. J.; Aquino, M. A. S.; White, C. A. *Can. J. Chem.* **1996**, *74*, 2201.

(66) Prasad, D. R.; Ferraudi, G. *Inorg. Chem.* **1983**, *22*, 1672.

(67) Rillema, D. P.; Nagle, J. K.; Barringer, L. F., Jr.; Meyer, T. J. *J. Am. Chem. Soc.* **1981**, *103*, 56. Harriman, A.; Porter, G.; Wilowska, A. *J. Chem. Soc., Faraday Trans. 2* **1983**, *79*, 807.

nate, or even reverse the electrostatic effect of the metal center but which do not provide a docking site for an acceptor such as MV^{2+}.

4.3. Supramolecular Assistance with Dicarboxylation. With a neutral, dicarboxylated complex such as $[Ru(\mathbf{1})_2(bpy)]^0$, the a priori expectation is that the electrostatically indifferent PET (neutral−dication encounter) will be advantaged over the electrostatically retarded BET (cation−cation encounter). Previous examples in aqueous solutions include $[Ru(bpy)_2(CN)_2]^0$, which showed 10-fold faster quenching of MV^{2+} than $[Ru(bpy)_3]^{2+}$ (at low salt concentration) despite a greater-than-2-fold deficit in τ, while $[Ru(dcbpy)(bpy)_2]^0$, with a somewhat lower τ than $[Ru(bpy)_3]^{2+}$, showed more than 4-fold faster quenching of MV^{2+} at a low salt concentration.[15]

In the present case of $[Ru(\mathbf{1})_2(bpy)]^0$, there was no activity in H_2O at all. This and its very weak luminescence suggest a very short τ for this species, one so short that the excited state does not appear to survive long enough to encounter any H_2O-solvated MV^{2+}, even if there is no electrostatic adversity in the encounter, and even though the efficiency of any successful encounters would be increased by electrostatically assisted photoproduct separation. This material was actually $[Ru(Na\mathbf{1})_2$-$(bpy)]^{2+}$, which, as a dication, would suffer the same electrostatic disadvantage as $[Ru(bpy)_3]^{2+}$, but the ready dissociation of Na^+ and cation exchange in H_2O should have easily overcome that impediment. (Only at high $[Na^+]$ might it interfere. This was seen with $[Ru(dcbpy)(bpy)_2]^0$, where the rates of quenching of MV^{2+} suffered a small negative salt effect that was attributed to a suppression by Na^+ of the interaction between the COO^- groups and MV^{2+}.)[15] The dissociation of Na^+ from $[Ru(Na\mathbf{1})_2$-$(bpy)]^{2+}$ would be less spontaneous in CH_3CN. An exchange with MV^{2+} would be entropically boosted but still more difficult than in H_2O. This and the poor luminescence makes the appreciable photoactivity of $[Ru(Na\mathbf{1})_2(bpy)]^{2+}$ in CH_3CN all the more remarkable and the enabling supramolecular interaction with MV^{2+} all the more important.

Indeed, if two peripheral COO^- groups are close enough to each other, their electrostatic fields can meld and a "two-point binding" of MV^{2+} can occur (Figure 5c). Such is the case with $[Ru^{II}(\mathbf{1})_2(bpy)]^0$, after the dissociation of Na^+ from $[Ru(Na\mathbf{1})_2$-$(bpy)]^{2+}$. The optimal interaction of MV^{2+} with $[Ru^{II}(\mathbf{1})_2(bpy)]^0$ will be side-on, to engage both charged nitrogens and both COO^- groups, but since the $COO^-\cdots COO^-$ separation in this example is somewhat greater than the $N\cdots N$ distance of MV^{2+}, the side-on guest will be offset from the symmetry axis to allow one end to be in especially intimate contact with one or the other COO^- group. A two-point interaction of this kind is understandably stronger than a one-point binding with mono-carboxylated sensitizers, and this is reflected in the calculated dissociation energies (Table 3). After PET, the two-point binding of the $MV^{\bullet+}$ photoproduct remains possible if we admit that resonance makes its two ends equivalent, but just as with the monocationic sensitizers, this binding is less secure than before PET and $MV^{\bullet+}$ is more vulnerable to cation exchange than was MV^{2+} before PET, as summarized by Scheme 3. In this particular case, $[Ru(Na\mathbf{1})_2(bpy)]^{2+}$ is already deprotonated ($HTEOA^+$ in this situation is not initially present and accumulates only through the deprotonation of $TEOA^{\bullet+}$, after reaction 2 in Scheme 1), but exchanges involving Na^+ (not depicted) can presumably play the same role as those involving

$HTEOA^+$. The combination of pre-PET association, unimolecular PET, and favorable post-PET exchanges accounts for the good level of photoactivity by $[Ru(Na\mathbf{1})_2(bpy)]^{2+}$ in CH_3CN despite an evidently very unfavorable τ value and the need to displace Na^+ ions.

$[Ru(\mathbf{8})_2]^0$ also presents a two-point binding site, albeit a little weaker because of the closer proximity of the metal (smaller s) and the wider splay of the two COO^- groups (larger r). Ligand $\mathbf{3}^{2-}$ also presents two COO^- groups on one side of the complex but is not amenable to two-point binding because the COO^- groups are too far apart and there is even some repulsive space between them (Figure 5b). $[Ru(\mathbf{7})_2]^0$ is the extreme case of this (Figure 5a). These latter two cases thus resemble monocarboxylated species with bigger bubbles: only one COO^- group can be intimately involved with any one $MV^{2+}/MV^{\bullet+}$, and only one $HTEOA^+$ is exchanged by $MV^{2+}/MV^{\bullet+}$ and *vice versa*. Indeed, the effect of the second carboxylation on k_f ($[Ru(\mathbf{7})_2]^0$ vs $[Ru(\mathbf{7})(ttpy)]^+$) was of the same order of magnitude as the effect of the first carboxylation ($[Ru(\mathbf{7})(ttpy)]^+$ vs $[Ru(ttpy)_2]^{2+}$); inasmuch as this one example is representative, this is consistent with the absence of any significant cooperativity.

The post-PET interaction between the photoproducts at close range will understandably be stronger with dicarboxylated sensitizers than with a singly carboxylated complex. This will be even more true with the tricarboxylated $[Ru(\mathbf{1})_3]^-$ and the tetracarboxylated $[Ru(\mathbf{3})_2]^{2-}$. In reflection of this, Table 1 reveals that generally higher k_q/k_f ratios were obtained with increasing levels of carboxylation.

4.4. Design Considerations. Our experimental results point out the general importance of electrostatics, solvent polarity, and excited-state lifetime, but it is difficult to draw detailed lessons on design. However, we can find confirmation of the general lessons and focus on some design details by examining the dependence of ΔG^* on its components. A desirable situation is obtained when the difference $\Delta\Delta G^* = \Delta G^*_{BET} - \Delta G^*_{PET}$ is optimally large and positive, and $\Delta\Delta G^*$ was largest with $[Ru(\mathbf{1})_2(bpy)]^0$, followed by $[Ru(\mathbf{1})(bpy)_2]^+$ (Table 4). To understand why and to determine the relative importance of the contributors to $\Delta\Delta G^*$, at least for those complexes listed in Table 4, we computed the derivatives $\delta\Delta\Delta G^*/\delta P$ for $P = E_{ox}$, E_{00}, ΔW, and Λ, where $\Delta W = W_P - W_R$, as well as the Λ components R_A and ρ (Supporting Information). The rank in terms of importance was not uniform throughout but was generally $\Delta W > \Lambda > E_{00} > E_{ox}$. $\delta\Delta\Delta G^*/\delta\Delta W$ ($= E_{00}/2\Lambda$) was uniformly the largest, confirming the preeminence of electrostatics among these factors. Its value hovered near $+1$, meaning that any increase in ΔW would immediately translate into a comparable increase in $\Delta\Delta G^*$. Indeed, as long as $\delta\Delta\Delta G^*/\delta\Delta W$ is > 0, which will hold whenever $\Lambda > 0$ (or $\rho > n^2$), then addressing the electrostatic situation as we have done will always be profitable. In this regard, ΔW was largest with $[Ru(\mathbf{1})_2(bpy)]^0$, smaller with $[Ru(\mathbf{8})_2]^0$, and smaller still with $[Ru(\mathbf{7})_2]^0$ because of less favorable r and s values. The singly carboxylated $[Ru(\mathbf{7})(ttpy)]^+$ actually fared better than $[Ru(\mathbf{7})_2]^0$ and showed a larger ΔW than $[Ru(\mathbf{1})(bpy)_2]^+$ or $[Ru(\mathbf{8})(H\mathbf{8})]^+$, because the difference between W_P and W_R fades with decreasing s.

Increasing E_{00} is also always helpful, and $\delta\Delta\Delta G^*/\delta E_{00}$ was highest when E_{00} was low. The importance of E_{ox} increases with E_{00}. Increasing E_{ox} is helpful except when Λ is high, which occurs when s is high (e.g., with ligand $\mathbf{7}^-$).

The effect of solvent is well summarized by $\delta\Delta\Delta G^*/\delta\rho$ and confirms the experimental findings. This derivative was small ($<\pm 0.006$), slightly positive with $[Ru(bpy)_3]^{2+}$ and $[Ru(ttpy)_2]^{2+}$ but negative with the carboxylated complexes. The $\delta\Delta\Delta G^*/\delta\Lambda \times \delta\Lambda/\delta\rho$ component was universally negative and near -0.001 in value, indicating the general benefit of a lower dielectric constant through a favorable change in Λ that would result. The $\delta\Delta\Delta G^*/\delta W \times \delta W/\delta\rho$ component was positive with $[Ru(bpy)_3]^{2+}$ and $[Ru(ttpy)_2]^{2+}$ but negative otherwise and largest with the dicarboxylated species. Thus, increasing ρ would benefit the dicationic complexes by making the unfavorable ΔW less negative, but for the carboxylated complexes, increasing ρ would be detrimental to ΔW and $\Delta\Delta G^*$. Finally, $\delta\Delta\Delta G^*/\delta R_A$ was dominated by the $\delta\Delta\Delta G^*/\delta\Lambda \times \delta\Lambda/\delta R_A$ component. $\delta\Delta W/\delta R_A$ was universally positive, as expected, but surprisingly much weaker than $\delta\Lambda/\delta R_A$. In the end, $\delta\Delta\Delta G^*/\delta R_A$ was strongest with ligands ttpy and bpy, weaker with H**8**, slightly negative with H**1**, and more so with H**7**, indicating that an R_A value near 8 Å (s near 6.5 Å) gives an optimal Λ.

Overall, our analysis of ΔG^* corroborates our experimental evidence of the benefits of carboxylation and may be similarly applicable to sensitizers anchored to semiconductor surfaces through peripheral anionic groups. Ideally, carboxylation should leave E_{ox} and E_{00} unaffected; that is, the carboxyl groups should not be π active. Phenylene linkers (as in H**7**), which prefer to remain unconjugated with the metal-binding site, are well suited for this, while direct, untethered carboxylation of the metal-binding domain (as in H**8** or in carboxybipyridines) may adversely increase E_{ox}, cause a red shift of λ_{max}, and depress E_{00}. As discussed earlier, untethered carboxyl groups can moreover adversely affect τ. The position of carboxylation (value of s) is important (especially to Λ) and should be neither too close to the metal (decreasing ΔW) nor too far (increasing Λ). Dicarboxylation with a suitable r value (carboxyl–carboxyl separation) enables two-point binding that translates to a larger ΔW and a larger $\Delta\Delta G^*$. As discussed in section 3.3, additional carboxyl groups bring smaller benefits, depending largely upon their proximity. Finally, less polar solvents are best with carboxylated sensitizers, favorably affecting both ΔW and Λ.

4,4′-Dicarboxypyridine complexes have been extensively used in photovoltaic devices.[47] They enjoy a very favorable r value but a relatively short s value (see section 2.4), and the computed ΔW and Λ values for $[Ru(dcbpy)(bpy)_2]^0$ (Table 4) are nearly identical to those of $[Ru(\mathbf{1})_2(bpy)]^0$. Its E_{ox} value is nearly the same as that for $[Ru(bpy)_3]^{2+}$ (1.27 V vs SCE), and its emission in CH_3CN occurs at 604 nm,[42] between those of $[Ru(bpy)_3]^{2+}$ and $[Ru(ttpy)_2]^{2+}$. $\Delta\Delta G^*$ for this complex is a little lower than that for $[Ru(\mathbf{1})_2(bpy)]^0$, but it has a sizable τ value (630 ns in CH_3CN)[42] that makes it a good candidate for PET in homogeneous solution. Without having performed the same treatment for the 3,3′, 5,5′- or 6,6′-dicarboxylated analogues, one can predict that their $\Delta\Delta G^*$ values will be substantially lower owing to much less appropriate r values in the first two cases and to inaccessibility in the 6,6′ case.

We found a correlation between the computed ΔG^* and the measured rate constants k_f and k_{init} for the nonluminescent complexes, but the effects on ΔG^* discussed previously combine with other effects, including the lifetime of luminescent species, to determine electron-transfer rates. By quantum mechanical theory, one of the pre-exponential terms is the electronic coupling factor.[35] The quality of the electronic overlap between reactants will vary with the sensitizer in a manner difficult to predict, perhaps according to the angle of approach which can be different for each sensitizer, viz. end-on for $[Ru(bpy)_3]^{2+}$ and side-on for $[Ru(\mathbf{1})_2(bpy)]^0$. The coupling factor has an exponential inverse relation to distance; sensitizers with lower s values (Table 2) would thus be at an advantage, but this would be true for both PET and BET. However, we can expect that the two-point-binding host sensitizers will enjoy a combination of unimolecular PET at short range and bimolecular BET at relatively longer mean distances.

5. Conclusion

The photochemical methodology used here is a convenient means of assessing sensitizers of wide-ranging abilities. This has highlighted the importance and benefit of short-range, supramolecular interactions in nonaqueous media. We found that even one peripheral COO^- group renders PET electrostatically more favorable than BET and enables supramolecular preassociation for enhanced PET rates, while two suitably disposed COO^- groups enable a stronger, two-point binding of MV^{2+} and an even more favorable electrostatic situation. Strong binding can also enhance the BET rates. Nevertheless, preassociation, along with favorable cation exchange pathways, accounts for the significant improvements in the rates of $MV^{\bullet+}$ generation with carboxylated complexes, though the fundamental photophysical properties remain important determinants of activity, especially when bimolecular PET is prevalent. The pyrazole-containing ligands of Chart 1 are evidently poor effectors of photoactivity, even with electrostatic assistance, likely because of extremely short excited-state lifetimes.

Supporting Information Available: Characterization data for the new complexes. Energy level diagrams analogous to Schemes 2 and 3 for complexes of ligands H$_2$**3**, H**7**, and H**8**. Derivation of the equations for F and E. Table of angles θ to accompany Table 3. Table of E, ΔW, and θ at three values of d for complexes of $\mathbf{1}^-$. Table of calculated derivatives of $\Delta\Delta G^*$ (10 pages). ^{1}H NMR spectra of the complexes of H**7** (2 pages). This material is available free of charge via the Internet at http://pubs.acs.org.